

## Supplementary Information

### Electron Transport Kinetics for Viologen-containing Polypeptides with Varying Side Group Linker Spacing

AUTHORS: Alexandra D. Easley,<sup>a</sup> Cheng-Han Li,<sup>b</sup> Shih-Guo Li,<sup>b</sup> Tan P. Nguyen,<sup>b</sup> Kai-Hua Mick Kuo,<sup>b</sup> Karen L. Wooley,<sup>\*abc</sup> Daniel P. Tabor,<sup>\*b</sup> and Jodie Lutkenhaus<sup>\*ac</sup>

<sup>a</sup> *Department of Materials Science and Engineering, Texas A&M University, College Station, TX 77843, USA.*

<sup>b</sup> *Department of Chemistry, Texas A&M University, College Station, TX 77843, USA*

<sup>c</sup> *Artie McFerrin Department of Chemical Engineering, Texas A&M University, College Station, TX 77843, USA*

\* Corresponding author email addresses: [jodie.lutkenhaus@tamu.edu](mailto:jodie.lutkenhaus@tamu.edu), [daniel\\_tabor@tamu.edu](mailto:daniel_tabor@tamu.edu), [wooley@chem.tamu.edu](mailto:wooley@chem.tamu.edu)

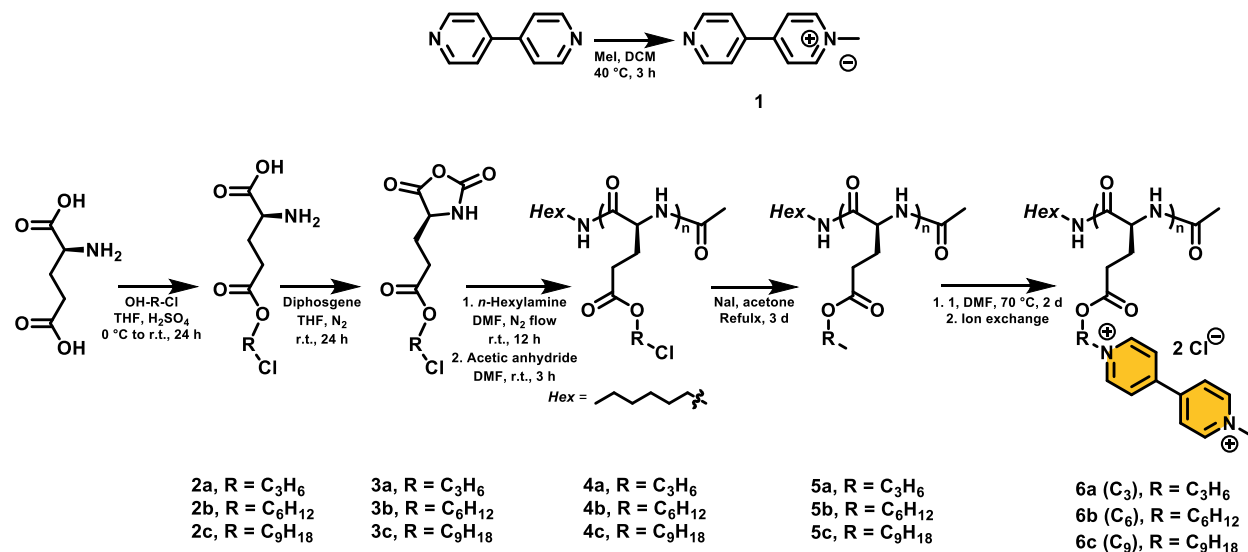
## Materials for synthesis of the viologen polypeptides and control viologen polymer

Acetonitrile (MeCN), 3,3-dithiodipropionic acid, 4,4'-dipyridine, dichloromethane (DCM), *N,N*-dimethylformamide (DMF), dimethylsulfoxide (DMSO), diphosgene, hexanes, *n*-hexylamine, iodomethane, 4-vinylbenzyl chloride (VBC), L-glutamic acid, methanol, sodium iodide (NaI), tetrahydrofuran (THF), and acetone were used as received from Sigma Aldrich. 3-Chloro-1-propanol was purchased from TCI chemicals and used as received. 6-Chloro-1-hexanol and acetic anhydride were purchased from Alfa-Aesar and used as received. 9-Chloro-1-nonanol was purchased from ChemScene (Monmouth Junction, NJ, USA) and used as received. 2,2'-Azobis(2-methylpropionitrile) (AIBN) was purchased from Sigma Aldrich and recrystallized from methanol before use. 4-Cyano-4-(((dodecylthio)carbonothioyl)thio)pentanoic acid (chain transfer agent, CTA) was used as received from Boron Molecular.

## Synthesis of the viologen polypeptides

The synthesis and spectral characterization of the viologen polypeptide with six carbon spacer (viologen polypeptide-C6, **6b**) was previously reported and is summarized in **Scheme S1**.<sup>1</sup>

**Scheme S1.** Synthesis of the C3, C6, and C9 viologen polypeptides.



### Synthesis of (3-Chloropropyl)-L-Glutamate (**2a**) and (9-Chlorononyl)-L-Glutamate (**2c**)

3-Chloro-1-propanol (7.5 mL, 0.090 mol) was added to a 250-mL round bottom flask charged with L-glutamic acid (5.0 g, 34 mmol). The mixture was cooled in an ice bath, followed by dropwise addition of sulfuric acid (2 mL). After warming to r.t., it was allowed to react for 24 h. Afterwards, ice-cold saturated aqueous sodium bicarbonate solution was slowly added to the reaction mixture. The product started to precipitate when the pH reached *ca.* 7 (monitored with pH paper).

The crude product was collected *via* filtration, dissolved in water/isopropanol (50 mL, 5/5, v/v) at 50 °C, hot filtered, and recrystallized at 4 °C to afford **2a** as a white solid (2.7 g, 12 mmol, 36%). <sup>1</sup>H NMR (400 MHz, TFA-*d*, ppm) δ 4.45 (dd, *J* = 6.1, 6.1 Hz, 1H), 4.35 (t, *J* = 6.1 Hz, 2H), 3.54 (t, *J* = 6.1 Hz, 2H), 2.83 (t, *J* = 6.6 Hz, 2H), 2.55 – 2.35 (m, 2H), 2.09 (quint, *J*<sub>12</sub> = 6.1 Hz, *J*<sub>23</sub> = 6.1 Hz, 2H). <sup>13</sup>C NMR (101 MHz, TFA-*d*, ppm) δ 176.36, 172.48, 63.68, 53.41, 39.47, 30.16, 29.95, 24.22. FTIR: 3300-2400, 1721, 1574, 1512, 1450, 1404, 1311, 1220, 1111, 1018, 957, 856, 764, 617 cm<sup>-1</sup>. MS (m/z) [M+H]<sup>+</sup> calc'd. 224.0684, found 224.0685.

(9-chlorononyl)-L-glutamate (**2c**) was synthesized using 9-chloro-1-nonanol and the same approach. Obtained 9.04 g (yield = 43%). <sup>1</sup>H NMR (400 MHz, TFA-*d*, ppm) δ 4.41 (dd, *J* = 7.0, 5.2 Hz, 1H), 4.14 (t, *J* = 6.8 Hz, 2H), 3.43 (t, *J* = 6.7 Hz, 2H), 2.78 (t, *J* = 6.6 Hz, 2H), 2.52 – 2.29 (m, 2H), 1.71 – 1.55 (m, 4H), 1.38 – 1.19 (m, 10H). <sup>13</sup>C NMR (101 MHz, TFA-*d*, ppm) δ 179.15, 174.96, 70.02, 55.89, 47.10, 34.42, 32.52, 31.06, 30.84, 30.54, 30.01, 28.57, 27.45, 26.73. FTIR: 3350-3130, 3130-2880, 2880-2675, 2675-2200, 1728, 1612, 1581, 1505, 1412, 1366, 1320, 1266, 1188, 1150, 1073, 1049, 995, 972, 880, 802, 756, 725, 648 cm<sup>-1</sup>. MS (m/z) [M+H]<sup>+</sup> calc'd. 308.1623, found 308.1620.

*Synthesis of (3-Chloropropyl)-L-Glutamate N-Carboxyanhydride (CPLG NCA, 3a) and (9-Chlorononyl)-L-Glutamate N-Carboxyanhydride (CNLG NCA, 3c)*

Inside an argon-filled glovebox, a 50-mL Schlenk flask was charged with **2a** (2.01 g, 8.99 mol) and anhydrous tetrahydrofuran (50 mL). The flask was then sealed, moved to a fume hood and placed under N<sub>2</sub> atmosphere, followed by dropwise addition of diphosgene (1.00 mL, 8.28 mmol) *via* a syringe. To protect the Schlenk line from contamination during the phosgenation reaction, a column charged with sodium hydroxide pellets was utilized to connect the Schlenk line and flask. **CAUTION: Phosgene and its derivatives are extremely hazardous. All manipulations must be performed using a reaction apparatus that provides for quenching phosgene that is released from the reaction set-up and is placed in a well-ventilated chemical fume hood with proper personal protective equipment and necessary precautions to avoid exposure.** After 24 h of reaction at r.t., the solvent was removed *in vacuo* using a double liquid nitrogen trap system where one trap was loaded with sodium hydroxide pellets. The concentrated oil was dissolved into ethyl acetate (50 mL) and washed with ice-cold aqueous media (water, saturated sodium bicarbonate × 2, brine and water, 50 mL each). The organic layer was dried over MgSO<sub>4</sub>, concentrated, and precipitated against hexanes (× 3) to afford **3a** as a yellow oil. The actual mass of **3a** was calculated by subtracting the mass of residual ethyl acetate from that of the collected oil, resulting in a yield of 1.23 g (4.93 mmol, 55%). The mole ratio between **3a** and ethyl acetate was calculated from <sup>1</sup>H NMR spectroscopy. <sup>1</sup>H NMR (400 MHz, CDCl<sub>3</sub>, ppm) δ 6.71 (s, 1H), 4.43 (dd, *J* = 5.5, 1.0 Hz, 1H), 4.27 (t, *J* = 6.1 Hz, 2H), 3.61 (t, *J* = 6.3 Hz, 2H), 2.57 (t, *J* = 6.9 Hz, 2H), 2.32 – 2.23 (m, 1H), 2.19 – 2.07 (m, 3H). <sup>13</sup>C NMR (101 MHz, CDCl<sub>3</sub>, ppm) δ 172.43, 169.37, 151.91, 61.97, 56.87, 41.04, 31.24, 29.53, 26.78. FTIR: 3460-3090, 3090-2800, 1854, 1776, 1728, 1360, 1244, 1171, 1103, 1045, 972, 918, 918, 756, 631 cm<sup>-1</sup>. MS (m/z) [M-H]<sup>-</sup> calc'd. 248.0320, found 248.0329.

(9-chlorononyl)-L-glutamate *N*-carboxyanhydride (CNLG NCA, **3c**) was synthesized using the same approach. Obtained 0.68 g (yield = 63%). <sup>1</sup>H NMR (400 MHz, CDCl<sub>3</sub>, ppm) δ 6.49 (s, 1H), 4.40 (dd, *J* = 5.2, 1.0 Hz, 1H), 4.09 (t, *J* = 6.8 Hz, 2H), 3.53 (t, *J* = 6.7 Hz, 2H), 2.55 (t, *J* = 6.3 Hz, 2H), 2.34-2.21 (m, 1H), 2.16-2.04 (m, 1H), 1.82 – 1.70 (m, 2H), 1.63 (m, 2H), 1.47 – 1.38 (m, 2H), 1.35 – 1.25 (m, 8H). <sup>13</sup>C NMR (101 MHz, CDCl<sub>3</sub>, ppm) δ 172.73, 169.37, 151.59, 65.49, 57.07, 45.15, 32.55, 29.93, 29.25, 29.05, 28.73, 28.43, 26.95, 26.78, 25.78. FTIR: 3450-3100, 3100-2880, 2880-2700, 1852, 1767, 1713, 1366, 1335, 1250, 1180, 1111, 1072, 934, 802, 748, 601 cm<sup>-1</sup>. MS (m/z) [M-H]<sup>-</sup> calc'd. 332.1259, found 332.1273.

*Synthesis of Poly((3-Chloropropyl)-L-Glutamate)<sub>50</sub> (PCPLG<sub>50</sub>, **4a**) and Poly((9-Chlorononyl)-L-Glutamate)<sub>50</sub> (PCNLG<sub>50</sub>, **4c**)*

Inside an argon-filled glovebox, a flame-dried 25-mL Schlenk flask was charged with the monomer **3a** (0.65 g, 2.6 mmol), dry DMF (7 mL) and a solution of hexylamine (145 μL, 0.36 mmol·mL<sup>-1</sup> in dry DMF, 0.052 mmol, monomer:initiator = 50:1). The reaction flask was then sealed, moved to a fume hood and connected to a Schlenk line through a N<sub>2</sub> flowmeter with a drierite column as an N<sub>2</sub> outlet. The reaction was stirred for 12 h under 100 mL·min<sup>-1</sup> N<sub>2</sub> flow at r.t. and monitored using FTIR spectroscopy. When the reaction was complete, the mixture was concentrated *in vacuo*, dissolved into DCM (10 mL), and precipitated into ice-cold methanol thrice to afford **4a** as a waxy white solid (0.35 g, 63%). <sup>1</sup>H NMR (400 MHz, CDCl<sub>3</sub>/TFA-*d*, 2/1, v/v, ppm) δ 4.62 (m), 4.37 – 4.10 (m), 3.57 (m), 2.53 (m), 2.23 – 1.92 (m), 0.87 (b). <sup>13</sup>C NMR (101 MHz, CDCl<sub>3</sub>/TFA-*d*, 2/1, v/v, ppm) δ 175.86, 173.38, 63.52, 53.53, 40.71, 31.02, 30.23, 27.17. FTIR: 3400-3130, 3130-3010, 3010-2750, 1786, 1730, 1661, 1548, 1502, 1439, 1385, 1256, 1090, 920, 864, 791, 760, 658 cm<sup>-1</sup>. The polymer exhibited an onset degradation temperature of *ca.* 309 °C and a glass transition temperature (*T*<sub>g</sub>) of *ca.* 46 °C. Elemental analysis results are provided in **Table S1**.

Poly((9-chlorononyl)-L-glutamate)<sub>50</sub> (PCNLG<sub>50</sub>, **4c**) was synthesized using the same approach. Obtained 0.20 g (yield = 76%). <sup>1</sup>H NMR (400 MHz, TFA-*d*, ppm) δ 4.75 (m), 4.18 (m), 3.50 (m), 2.59 (m), 2.34 – 2.21 (m), 2.18-2.01 (m), 1.80 – 1.63 (m), 1.49-1.23 (m), 0.85 (b). <sup>13</sup>C NMR (101 MHz, TFA-*d*, ppm) δ 178.71, 175.81, 69.41, 55.77, 46.92, 34.49, 32.35, 31.17, 30.97, 30.64, 30.14, 29.22, 28.66, 27.49. FTIR: 3410-3130, 3130-3020, 3020-2880, 2880-2700, 1728, 1651, 1543, 1450, 1319, 1250, 1165, 1080, 1018, 964, 926, 733, 694, 610 cm<sup>-1</sup>. The polymer exhibited an onset degradation temperature of *ca.* 315 °C and a *T*<sub>g</sub> of *ca.* -52 °C. Elemental analysis results are provided in **Table S1**.

*Synthesis of Poly((3-Iodopropyl)-L-Glutamate)<sub>50</sub> (PIPLG<sub>50</sub>, **5a**) and Poly((9-Iodononyl)-L-Glutamate)<sub>50</sub> (PINLG<sub>50</sub>, **5c**)*

Poly((3-chlorohexyl)-L-glutamate)<sub>50</sub> (**4a**, 0.13 g, 0.62 mmol) and NaI (0.98 g, 6.6 mmol) were added into a 25-mL round bottom flask charged with acetone (12 mL). The reaction was stirred for 3 d while being heated at reflux and monitored by <sup>1</sup>H NMR spectroscopy. Upon completion, the solvent was evaporated, followed by the addition of chloroform (12 mL). The chloroform

solution was then stored at 4 °C for 12 h to precipitate residual NaI, which was then removed *via* gravity filtration. The filtrate was washed with ice-cold water (12 mL × 3), dried over MgSO<sub>4</sub>, and evaporated *in vacuo* to obtain **5a** as a yellow wax (90 mg, 49%). <sup>1</sup>H NMR (400 MHz, CDCl<sub>3</sub>/TFA-*d*, 2/1, v/v, ppm) δ 4.54 (m), 4.20 (m), 3.18 (m), 2.51 (m), 2.25 – 1.91 (m), 0.87 (b). <sup>13</sup>C NMR (101 MHz, CD<sub>3</sub>Cl<sub>3</sub>/TFA-*d*, 2/1, v/v, ppm) δ 175.32, 173.41, 66.17, 53.77, 31.80, 30.24, 26.80, 0.42. FTIR: 3410-3120, 3120-3010, 3010-2680, 1728, 1651, 1543, 1442, 1389, 1315, 1242, 1165, 1118, 1088, 1026, 996, 840, 794, 724, 609 cm<sup>-1</sup>. The polymer exhibited an onset degradation temperature of *ca.* 268 °C and a *T<sub>g</sub>* of *ca.* 51 °C. Elemental analysis results are provided in **Table S1**.

Poly((9-iodononyl)-L-glutamate)<sub>50</sub> (PINLG<sub>50</sub>, **5c**) was synthesized using the same approach. Obtained 0.12 g (yield = 63%). <sup>1</sup>H NMR (400 MHz, CDCl<sub>3</sub>/TFA-*d*, 2/1, v/v, ppm) δ 4.58 (m), 4.08 (m), 3.19 (m), 2.48 (m), 2.19 – 2.04 (m), 1.95 (m), 1.81 (m), 1.60 (m), 1.43 – 1.22 (m), 0.87 (b). <sup>13</sup>C NMR (101 MHz, CD<sub>3</sub>Cl<sub>3</sub>/TFA-*d*, 2/1, v/v, ppm) δ 175.86, 173.21, 66.88, 53.35, 33.68, 30.59, 30.21, 27.08, 29.39, 29.22, 28.59, 28.26, 25.67, 7.26. FTIR: 3410-3130, 3130-3010, 3010-2880, 2880-2680, 1728, 1651, 1543, 1450, 1394, 1319, 1243, 1173, 1118, 1080, 1003, 795, 718, 602 cm<sup>-1</sup>. The polymer exhibited an onset degradation temperature of *ca.* 270 °C and a *T<sub>g</sub>* of *ca.* -50 °C. Elemental analysis results are provided in **Table S1**.

#### *Synthesis of Poly((3-Iodo)-L-Glutamate)-g-Methyl Viologen (Viologen Polypeptide-C3, **6a**) and Poly((9-Iodo)-L-Glutamate)-g-Methyl Viologen (Viologen Polypeptide-C9, **6c**)*

Typically, inside an argon-filled glovebox, **5a** (0.084 g, 0.28 mmol) and **1** (0.85 g, 2.8 mmol) were added into a 100-mL Schlenk flask charged with dry DMF (8 mL). The reaction was stirred for 2 d at 70 °C under N<sub>2</sub> atmosphere. Upon completion, the reaction mixture was dialyzed with a membrane (molecular weight cutoff of 3500 g/mol) against nanopure water for 3 d and the resulting aqueous solution remaining in the dialysis tubing was lyophilized to obtain the viologen-iodide (viol-I) polypeptide (**6a-I**) as a reddish brown solid (0.14 g, 85%). The iodides in **6a-I** were exchanged using Dowex<sup>®</sup> A2 ion exchange resin to obtain the viologen-chloride (viol-Cl) polypeptide (**6a-Cl**) as a dark brown solid. <sup>1</sup>H NMR (500 MHz, DMSO-*d*<sub>6</sub>, ppm) δ 9.56 – 9.39 (m), 9.39 – 9.26 (m), 8.90 – 8.74 (m), 8.24 – 8.00 (m), 5.03 – 4.71 (m), 4.55 – 4.43 (m), 4.37 – 3.98 (m), 2.46 – 2.26 (m), 2.08 – 1.63 (m). <sup>13</sup>C NMR (126 MHz, DMSO-*d*<sub>6</sub>, ppm) δ 172.34, 171.05, 148.64, 148.00, 146.59, 145.94, 126.61, 126.15, 60.94, 58.20, 51.71, 48.18, 31.05, 29.99, 27.28. FTIR: 3660-3300, 3300-3150, 3150-2560, 1721, 1636, 1528, 1443, 1343, 1263, 1165, 1074, 1034, 964, 818, 709, 602 cm<sup>-1</sup>. Polymer **6a-I** exhibited an onset degradation temperature of *ca.* 245 °C and a *T<sub>g</sub>* of *ca.* 145 °C. Polymer **6a-Cl** exhibited an onset degradation temperature of *ca.* 253 °C, but did not exhibit a *T<sub>g</sub>* value in the tested temperature window. Elemental analysis results are provided in **Table S1**.

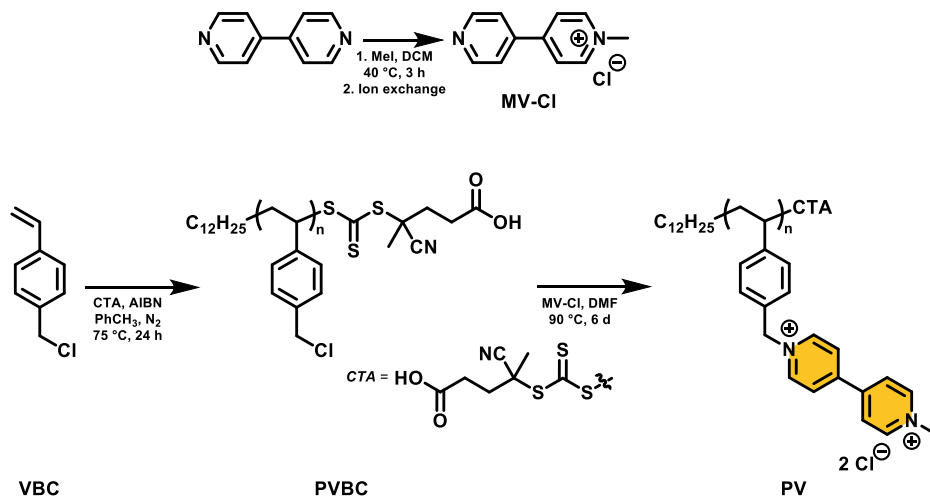
Poly((9-iodo)-L-glutamate)-g-methyl viologen (Viologen Polypeptide-C9, **6c**) was synthesized using the same approach. Obtained 0.16 g (yield = 78%). <sup>1</sup>H NMR (500 MHz, DMSO-*d*<sub>6</sub>, ppm) δ 9.54 – 9.37 (m), 9.36 – 9.25 (m), 8.89 – 8.72 (m), 8.27 – 7.81 (m), 4.85 – 4.63 (m), 4.55 – 4.38 (m), 4.37 – 4.12 (m), 4.11 – 3.82 (m), 2.39 – 2.21 (m), 2.05 – 1.94 (m), 1.92 – 1.70 (m), 1.60 –

1.47 (m), 1.41 – 1.16 (m).  $^{13}\text{C}$  NMR (126 MHz, DMSO- $d_6$ , ppm)  $\delta$  172.32, 170.80, 148.43, 148.05, 146.57, 145.68, 126.55, 126.11, 63.90, 60.76, 60.67, 48.12, 32.46, 30.81, 30.06, 28.81, 28.62, 28.42, 28.13, 25.49, 25.28. FTIR: 3640-3370, 3370-3150, 3150-2980, 2980-2880, 2880-2660, 1728, 1643, 1543, 1450, 1343, 1250, 1173, 818, 710, 610  $\text{cm}^{-1}$ . Polymer **6c-I** exhibited an onset degradation temperature of *ca.* 249 °C and a  $T_g$  of *ca.* 130 °C. Polymer **6c-Cl** exhibited an onset degradation temperature of *ca.* 220 °C, but did not exhibit a  $T_g$  value in the tested temperature window. Elemental analysis results are provided in **Table S1**.

### Synthesis of the control viologen polymer.

Poly(vinylbenzyl methyl viologen) was synthesized following a modified method as reported by Nagarjuna *et al* and summarized in **Scheme 2**.<sup>2</sup> First, methyl viologen chloride (**MV-Cl**) was synthesized following the procedure reported by Nguyen *et al*. followed by ion exchange with using Dowex® A2 ion exchange resin.<sup>1</sup> In parallel, poly(vinylbenzyl chloride) (**PVBC**) was synthesized *via* reversible addition–fragmentation chain-transfer (RAFT) polymerization.

**Scheme S2.** Synthesis of the control viologen polymer poly(vinylbenzyl methyl viologen) or PV.



### Synthesis of Poly(vinylbenzyl chloride) (**PVBC**)

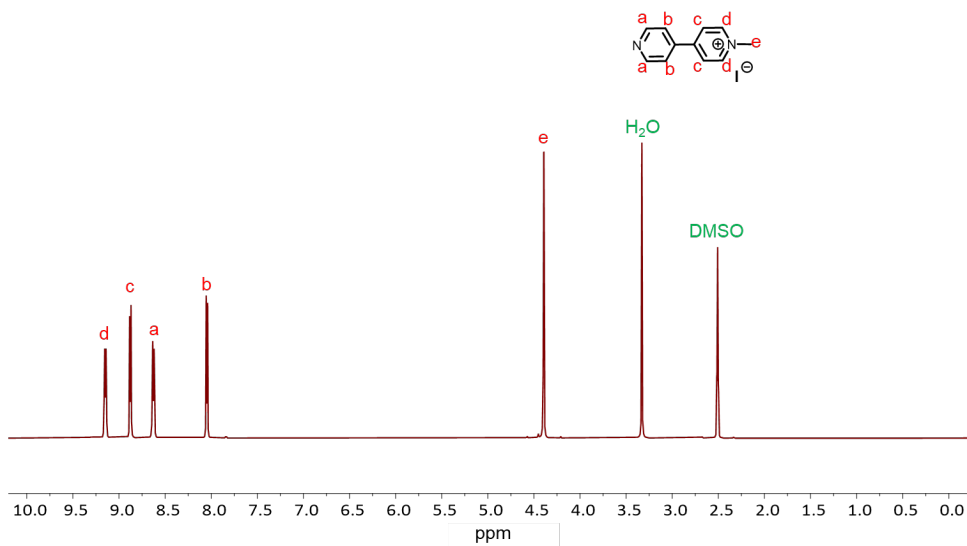
In a 25-mL Schlenk flask VBC (5.0 g, 32 mmol), AIBN (11 mg, 0.067 mmol), CTA (54 mg, 0.14 mmol), and 7.8 mL of toluene were combined at ambient conditions. Resulting in a monomer : initiator : CTA molar ratio of 228 : 0.5 : 1. The flask was then sealed and three freeze-pump-thaw cycles were carried out with N<sub>2</sub> gas and liquid N<sub>2</sub>. After the final thaw, the flask was sealed and heated to 75 °C allowed to react for 24 h. After 24 h, the reaction was cooled to room temperature and exposed to ambient air to terminate the reaction. The reaction solution was then precipitated in hexanes followed by washing with copious diethyl ether during filtration. The resulting **PVBC** was dried overnight at r.t. under vacuum to afford **PVBC** as a pale yellow solid (1.5 g, 30%). <sup>1</sup>H NMR (400 MHz, DMSO-*d*<sub>6</sub>, ppm) δ 7.12 (b), 6.51 (b), 4.66 (b), 2.20 – 1.10 (b). <sup>13</sup>C NMR (101 MHz, DMSO-*d*<sub>6</sub>, ppm) δ 145.52, 135.50, 129.12, 127.91, 46.65. FTIR: 3150-2990, 2990-2870, 2870-2740, 1910, 1611, 1510, 1432, 1262, 1110, 1018, 822, 740, 671 cm<sup>-1</sup>. **PVBC** exhibited an onset degradation temperature of *ca.* 343 °C and a *T*<sub>g</sub> of *ca.* 102 °C. Elemental analysis results are provided in **Table S1**.

*Synthesis of Poly(vinylbenzyl methyl viologen) or the control viologen polymer (PV)*

Following a procedure similar to Nagarjuna *et al*, **PVBC** (86 mg, 0.56 mmol of repeat unit, 1 equiv.), **MV-Cl** (0.58 g, 2.8 mmol, 5 equiv.), and 5.6 mL of dry DMF were combined in a 25-mL Schlenk flask equipped with a condenser.<sup>2</sup> The reaction was then heated to 90 °C and allowed to react for 6 d under an N<sub>2</sub> atmosphere. Upon completion, the reaction solution was dialyzed with a membrane (molecular weight cut off of 3500 g/mol) against nanopure water for 3 d. After lyophilization, poly(vinylbenzyl methyl viologen) (**PV**) was collected as a reddish solid (0.14 g, 70% isolated yield). <sup>1</sup>H NMR (400 MHz, DMSO-*d*<sub>6</sub>, ppm) δ 9.83 (b), 9.40 (b), 8.97 (b), 7.54 (b), 6.36 (b), 4.5 (b), 0.86 – 2.30 (b). <sup>13</sup>C NMR was attempted but provided unassignable spectra with high signal-to-noise ratio. FTIR: 3660-3140, 3140-3080, 3080-2950, 2950-2850, 1633, 1559, 1505, 1443, 1343, 1214, 1189, 1152, 1013, 814, 792, 702, 673-610 cm<sup>-1</sup>. **PV** exhibited an onset degradation temperature of *ca.* 202 °C, but did not exhibit a *T<sub>g</sub>* value in the tested temperature window. Elemental analysis results are provided in **Table S1**.



400 MHz - DMSO- $d_6$



101 MHz - DMSO- $d_6$

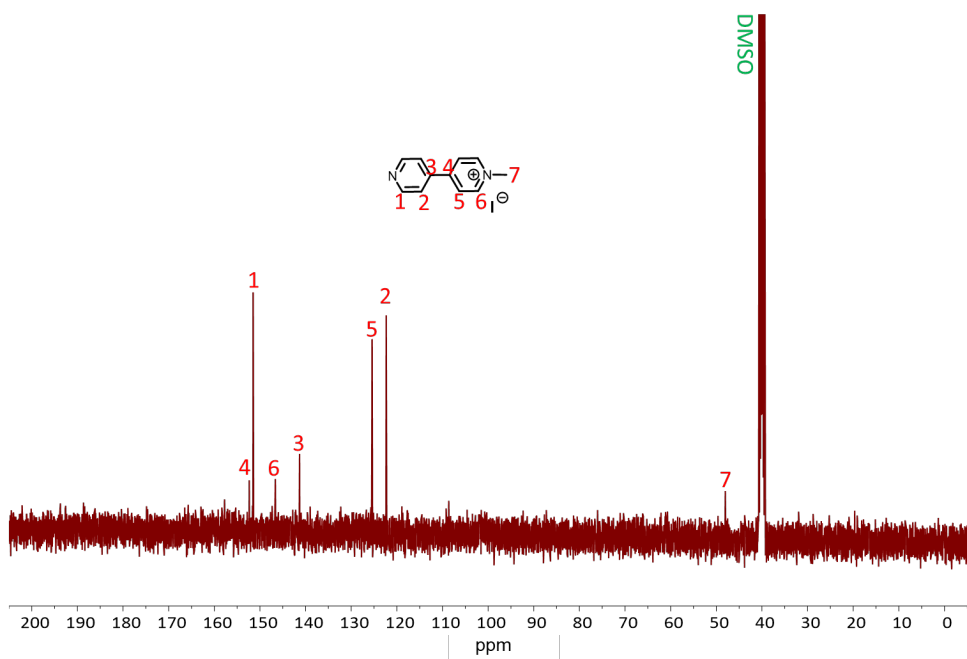
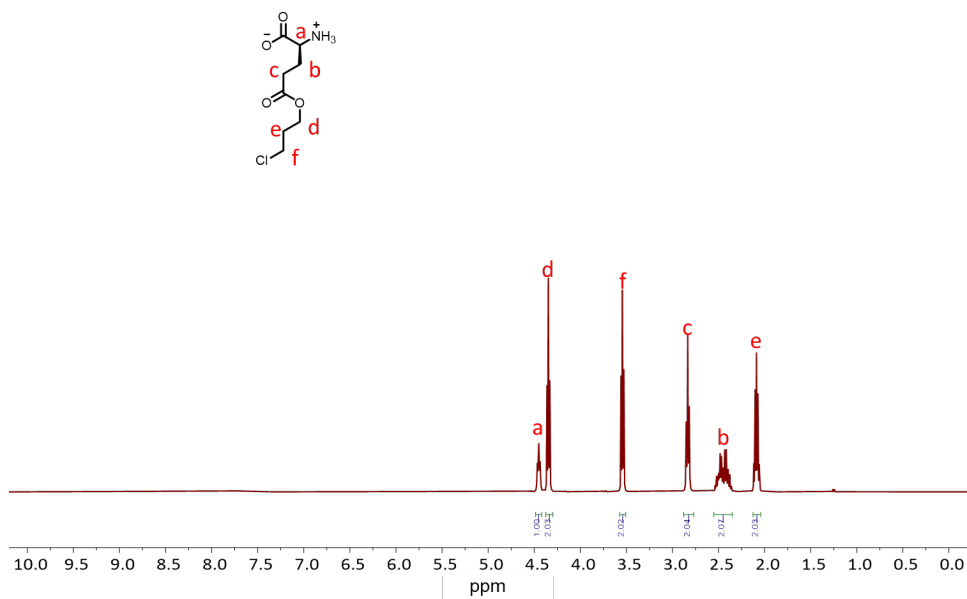


**Figure S1.**  $^1\text{H}$  NMR (400 MHz, DMSO- $d_6$ ) and  $^{13}\text{C}$  NMR (101 MHz, DMSO- $d_6$ ) spectra of MBPI (1).

400 MHz – TFA-*d*



101 MHz – TFA-*d*

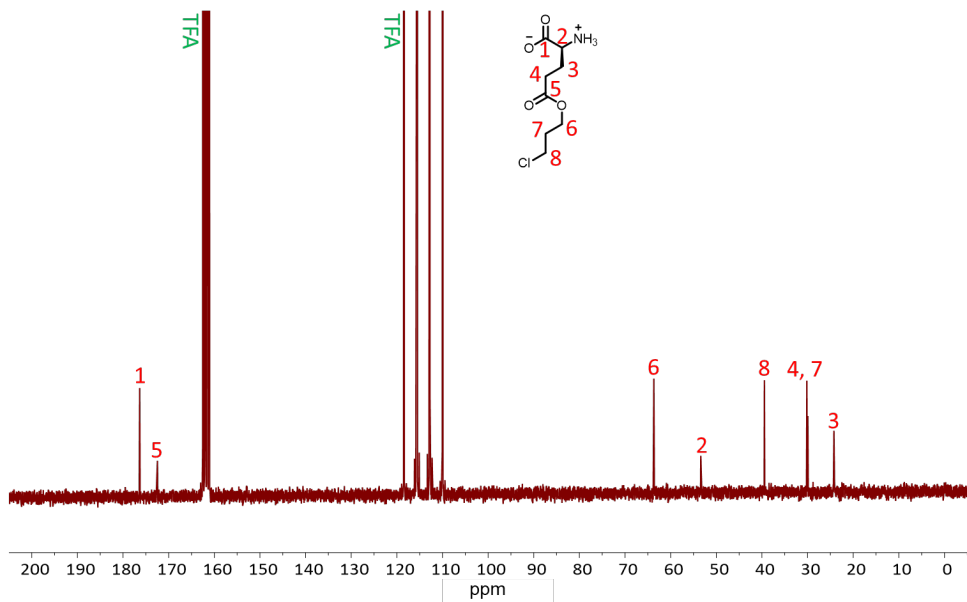
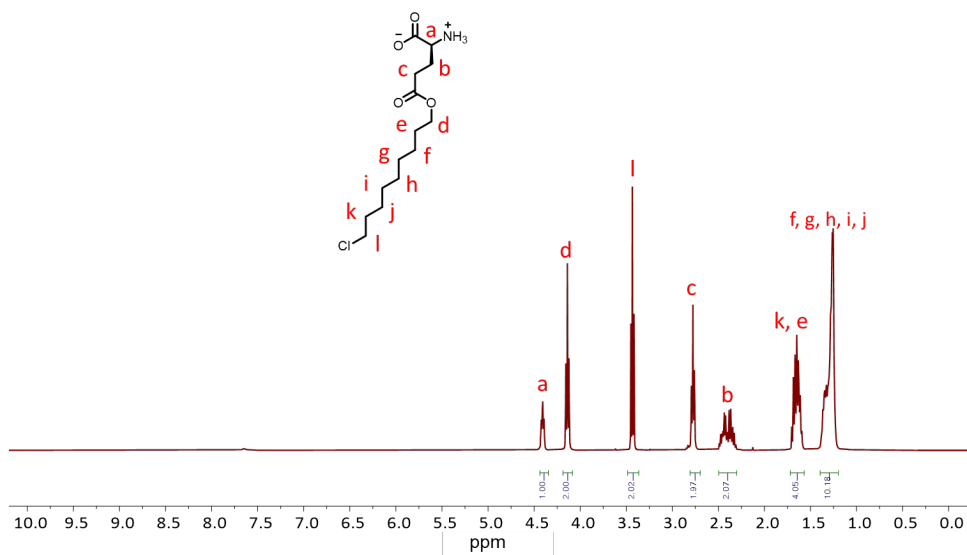


**Figure S2.** <sup>1</sup>H NMR (400 MHz, TFA-*d*) and <sup>13</sup>C NMR (101 MHz, TFA-*d*) spectra of CPLG (2a).

400 MHz - TFA-*d*



101 MHz - TFA-*d*

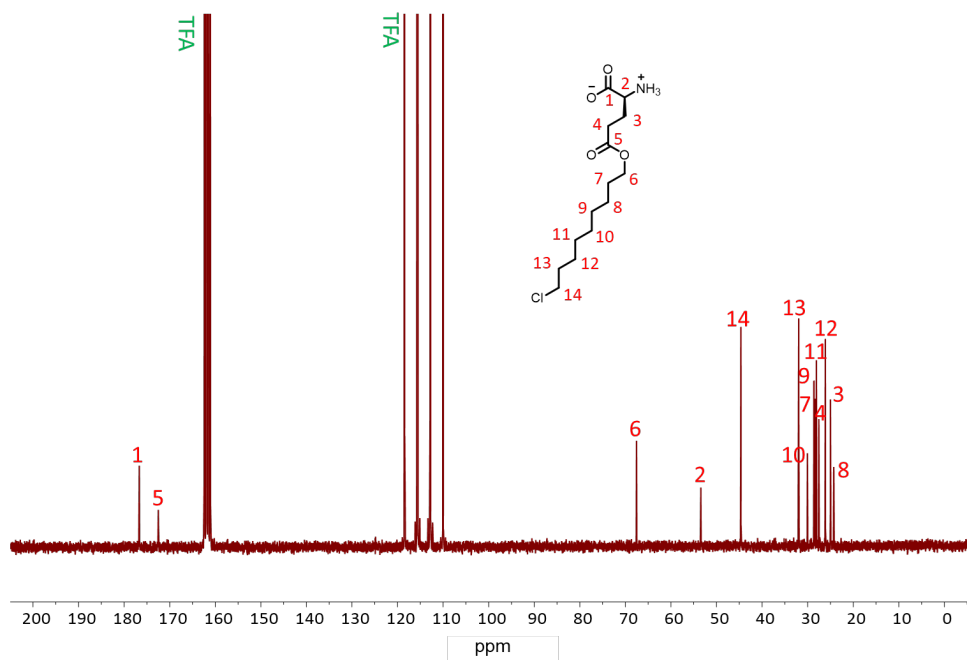
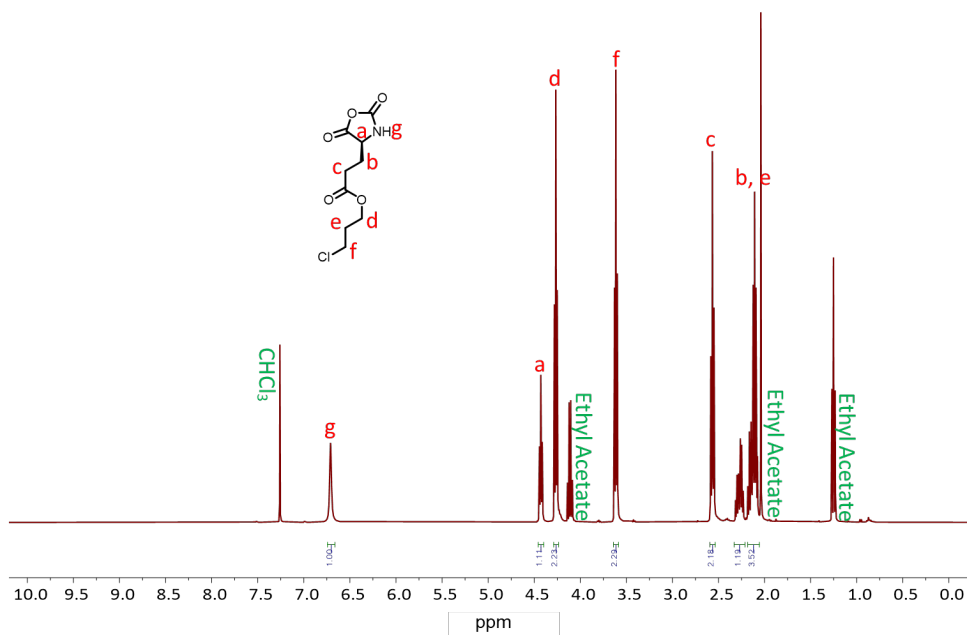


**Figure S3.**  $^1\text{H}$  NMR (400 MHz, TFA-*d*) and  $^{13}\text{C}$  NMR (101 MHz, TFA-*d*) spectra of CNLG (2c).

400 MHz – CDCl<sub>3</sub>



101 MHz – CDCl<sub>3</sub>

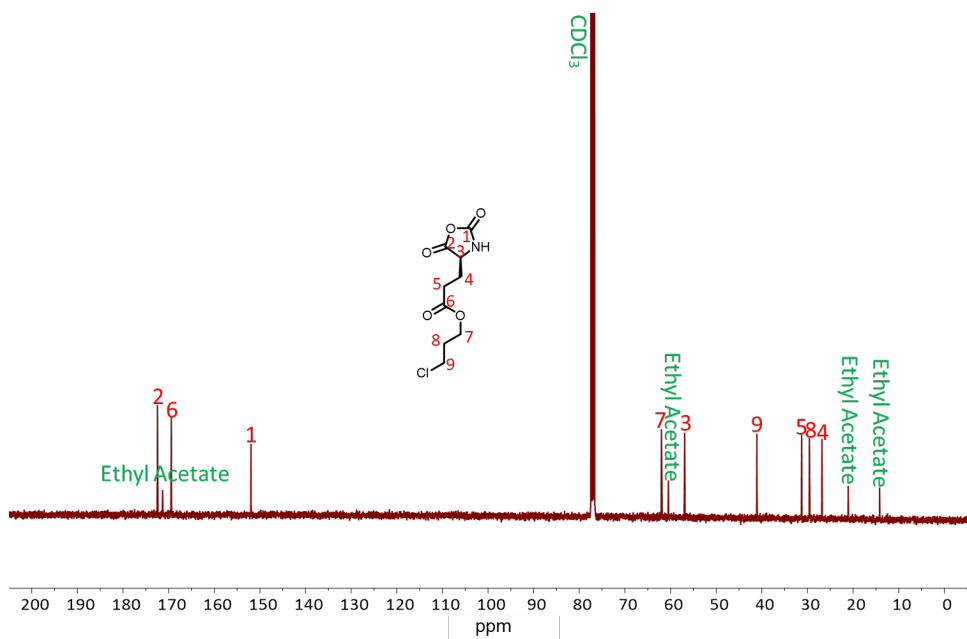
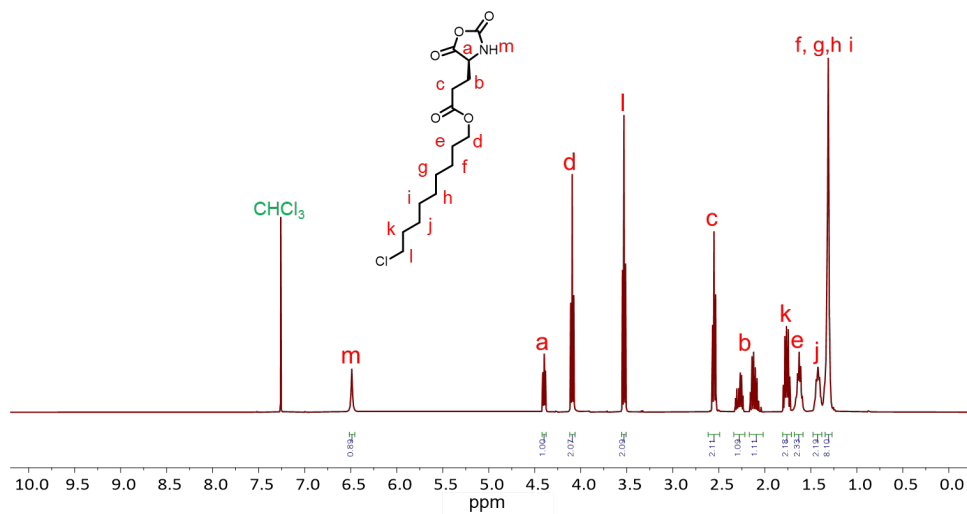


**Figure S4.** <sup>1</sup>H NMR (400 MHz, CDCl<sub>3</sub>) and <sup>13</sup>C NMR (101 MHz, CDCl<sub>3</sub>) spectra of CPLG NCA (**3a**).

400 MHz – CDCl<sub>3</sub>



101 MHz – CDCl<sub>3</sub>

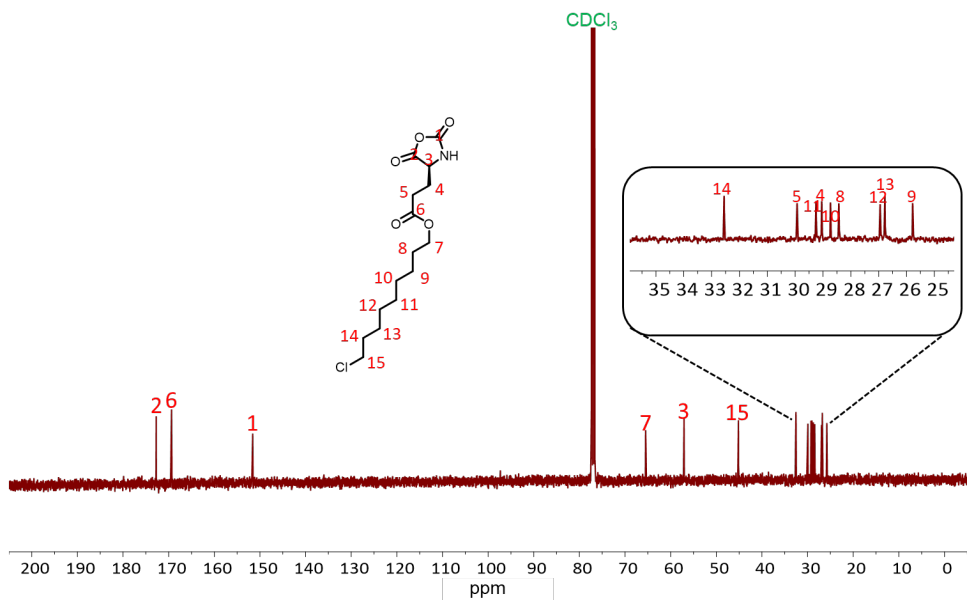
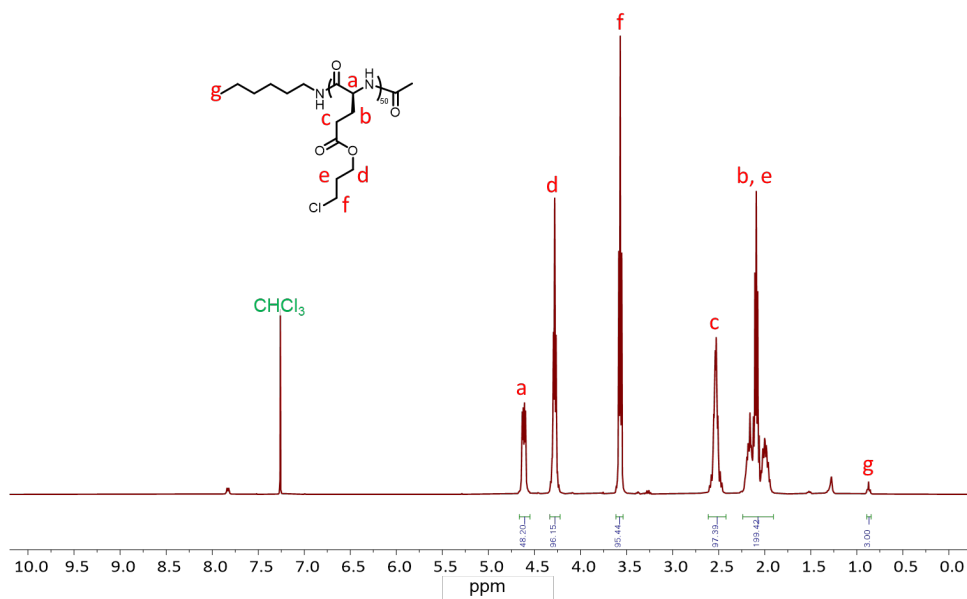


**Figure S5.** <sup>1</sup>H NMR (400 MHz, CDCl<sub>3</sub>) and <sup>13</sup>C NMR (101 MHz, CDCl<sub>3</sub>) spectra of CNLG NCA (3c).

400 MHz – CDCl<sub>3</sub>/TFA-*d* (2/1, v/v)



101 MHz – CDCl<sub>3</sub>/TFA-*d* (2/1, v/v)

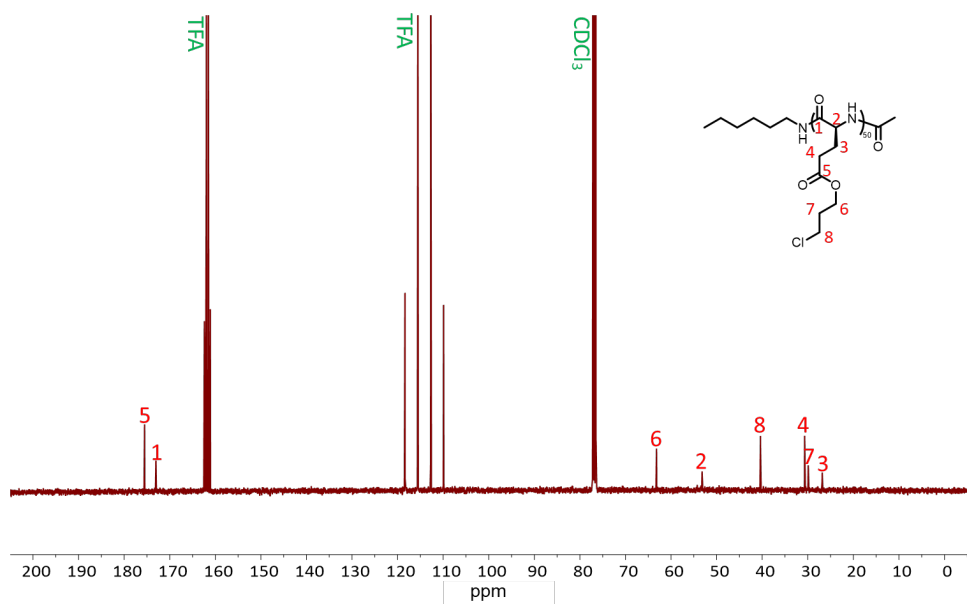
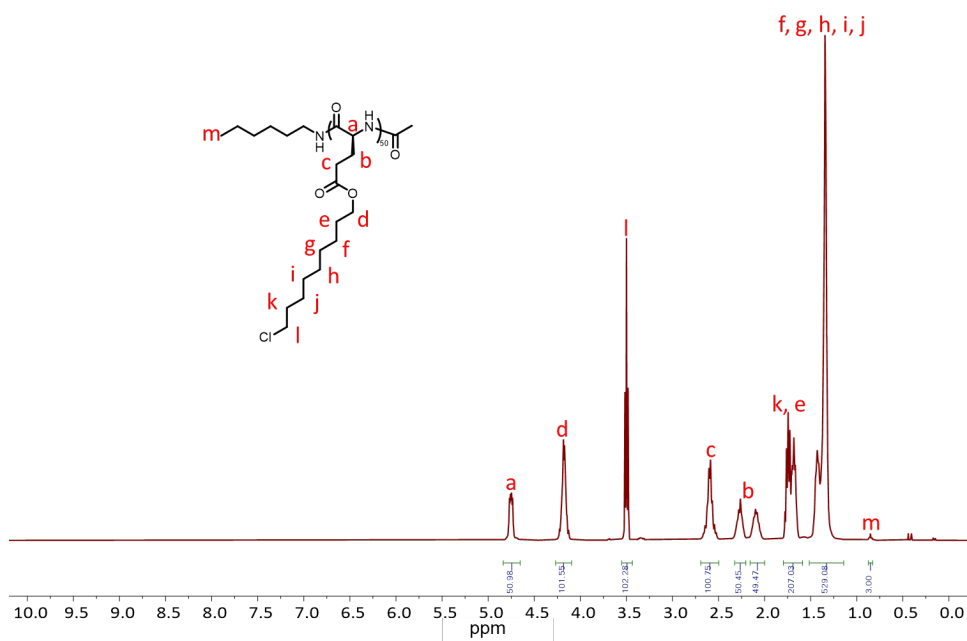


**Figure S6.** <sup>1</sup>H NMR (400 MHz, CDCl<sub>3</sub>/TFA-*d*, 2:1, v/v) and <sup>13</sup>C NMR (101 MHz, CDCl<sub>3</sub>/TFA-*d*, 2:1, v/v) spectra of PCPLG (**4a**).

400 MHz - TFA-*d*



101 MHz - TFA-*d*

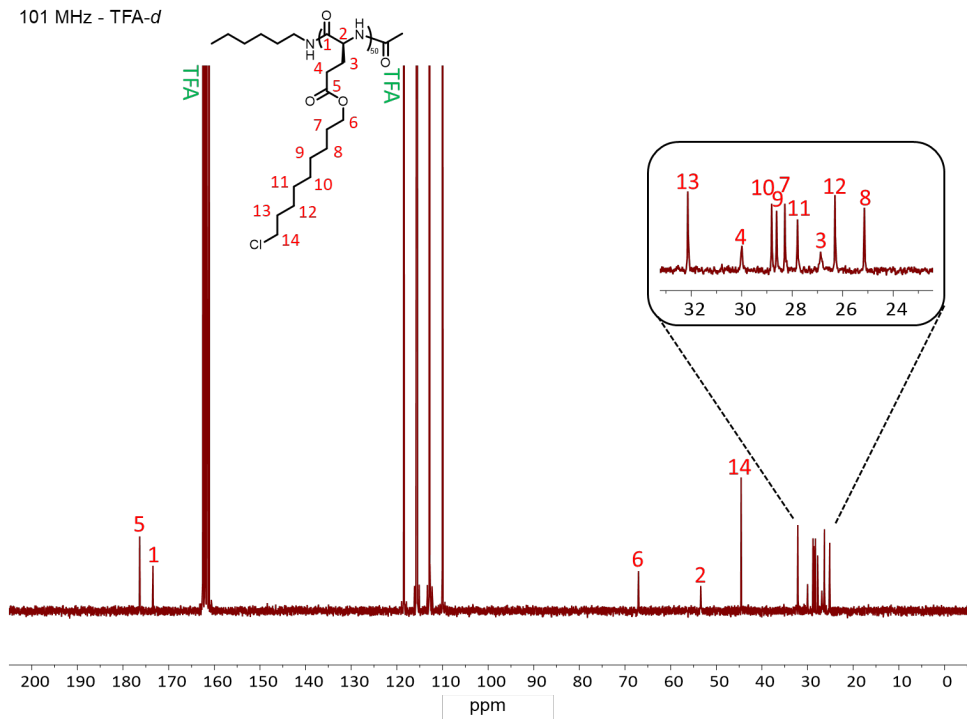
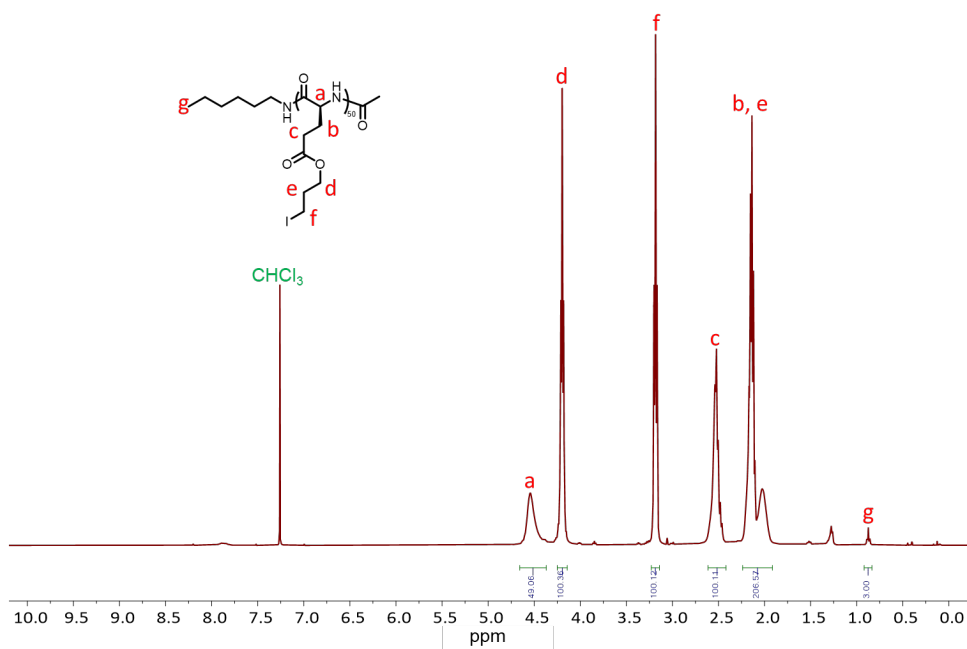


**Figure S7.** <sup>1</sup>H NMR (400 MHz, TFA-*d*) and <sup>13</sup>C NMR (101 MHz, TFA-*d*) spectra of PCNLG (4c).

400 MHz – CDCl<sub>3</sub>/TFA-*d* (2/1, v/v)



400 MHz – CDCl<sub>3</sub>/TFA-*d* (2/1, v/v)

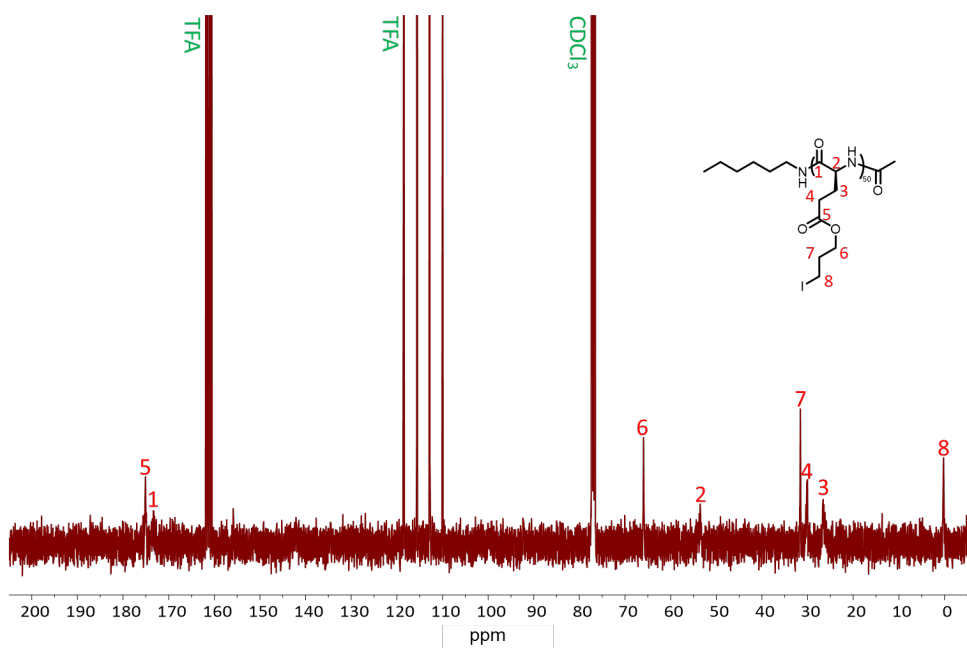
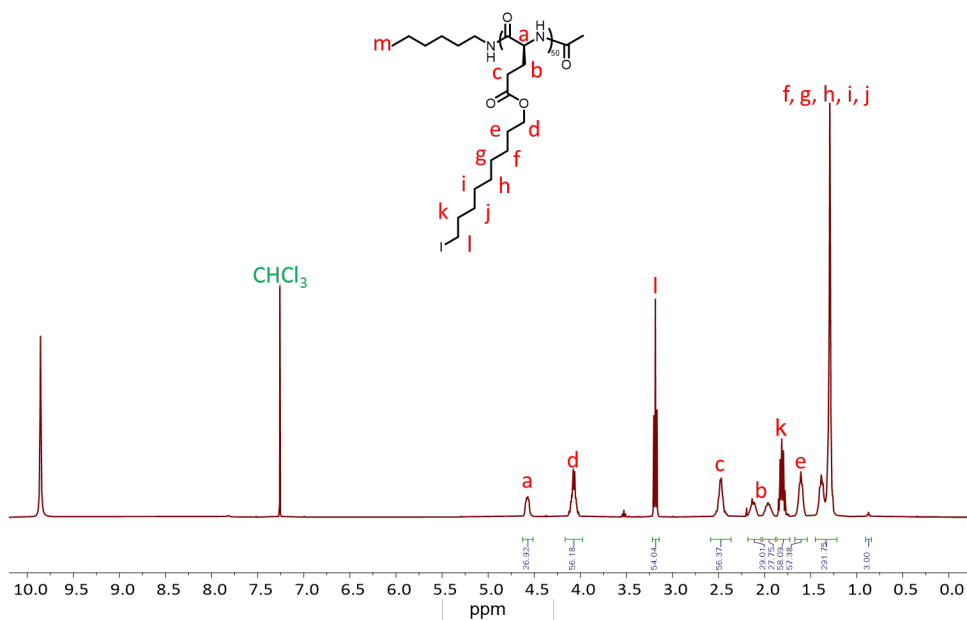


**Figure S8.** <sup>1</sup>H NMR (400 MHz, CDCl<sub>3</sub>/TFA-*d*, 2:1, v/v) and <sup>13</sup>C NMR (101 MHz, CDCl<sub>3</sub>/TFA-*d*, 2:1, v/v) spectra of PIPLG (**5a**).



400 MHz – CDCl<sub>3</sub>/TFA-*d* (2/1, v/v)



101 MHz – CDCl<sub>3</sub>/TFA-*d* (2/1, v/v)

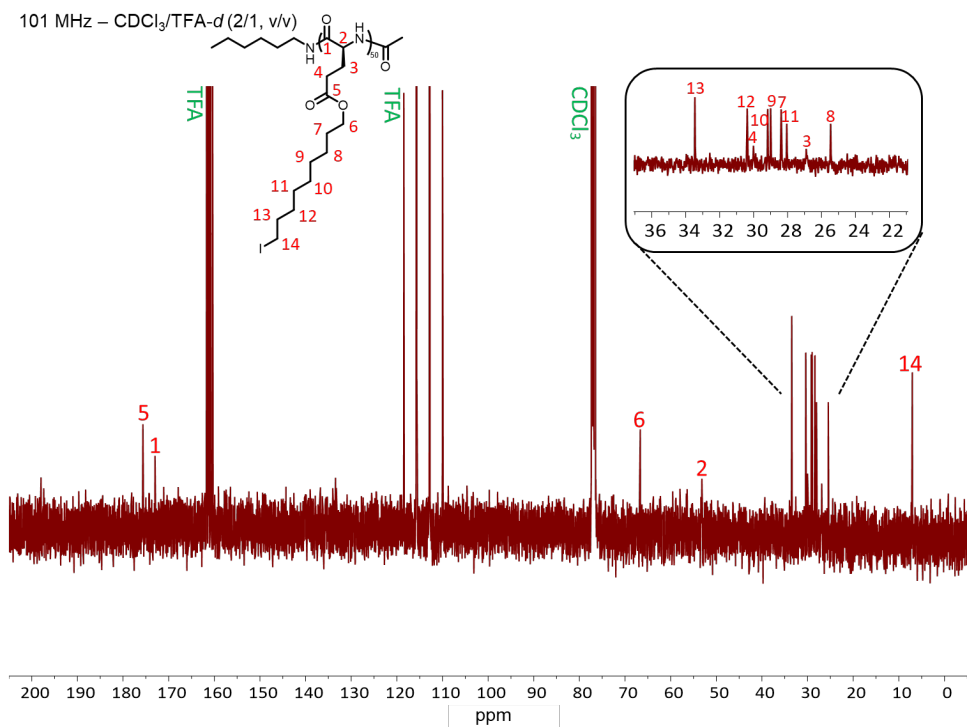
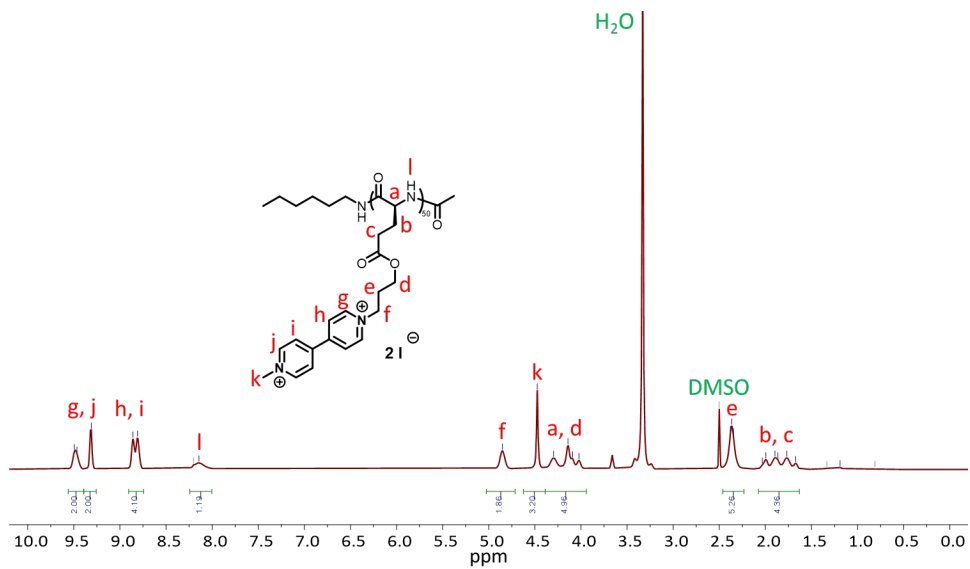


**Figure S9.** <sup>1</sup>H NMR (400 MHz, CDCl<sub>3</sub>/TFA-*d*, 2:1, v/v) and <sup>13</sup>C NMR (101 MHz, CDCl<sub>3</sub>/TFA-*d*, 2:1, v/v) NMR spectra of PINLG (5c).

500 MHz - DMSO- $d_6$



126 MHz - DMSO- $d_6$

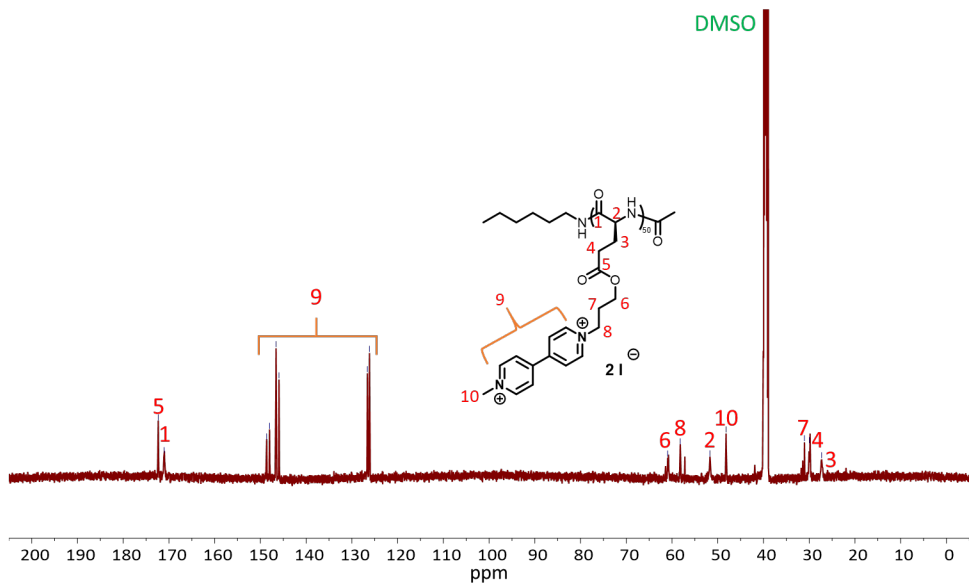
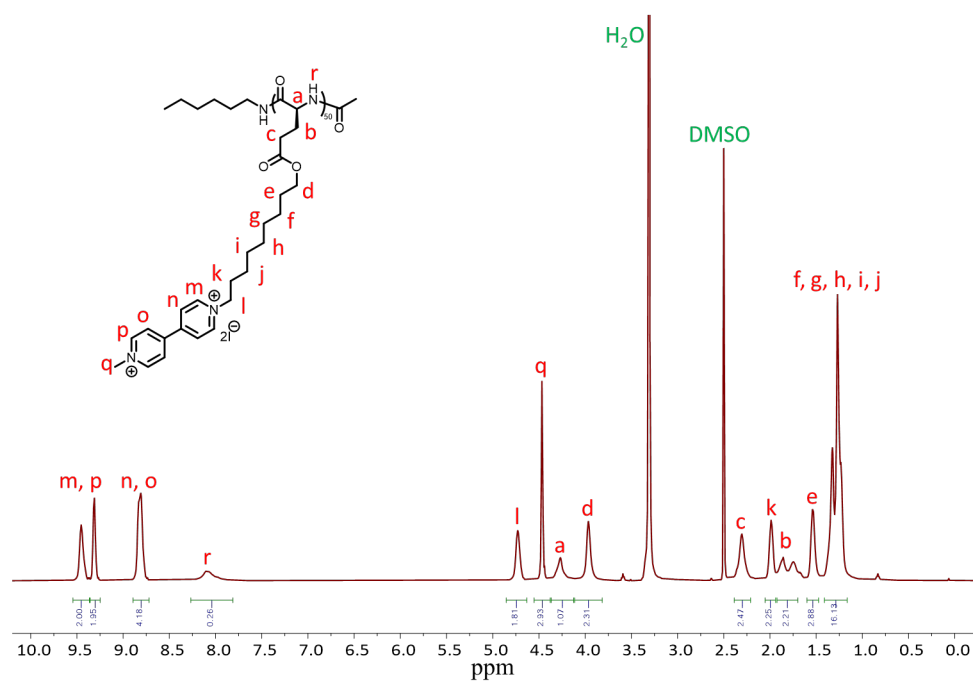


**Figure S10.**  $^1\text{H}$  NMR (500 MHz, DMSO- $d_6$ ) and  $^{13}\text{C}$  NMR (126 MHz, DMSO- $d_6$ ) spectra of Viologen Polypeptide-C3 (**6a**).

500 MHz - DMSO- $d_6$



126 MHz - DMSO- $d_6$

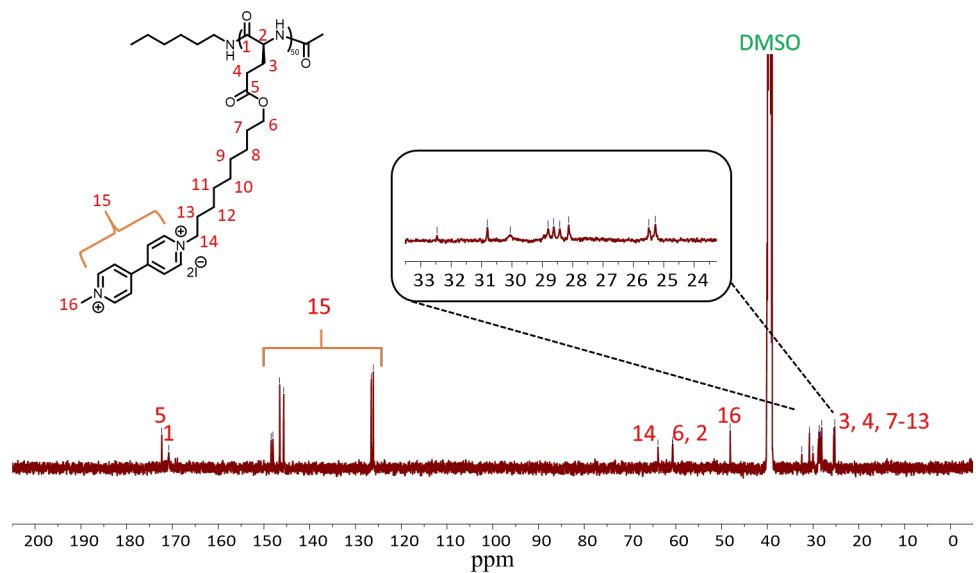


**Figure S11.**  $^1\text{H}$  NMR (500 MHz, DMSO- $d_6$ ) and  $^{13}\text{C}$  NMR (126 MHz, DMSO- $d_6$ ) spectra of Viologen Polypeptide-C9 (6c).

400 MHz - DMSO- $d_6$

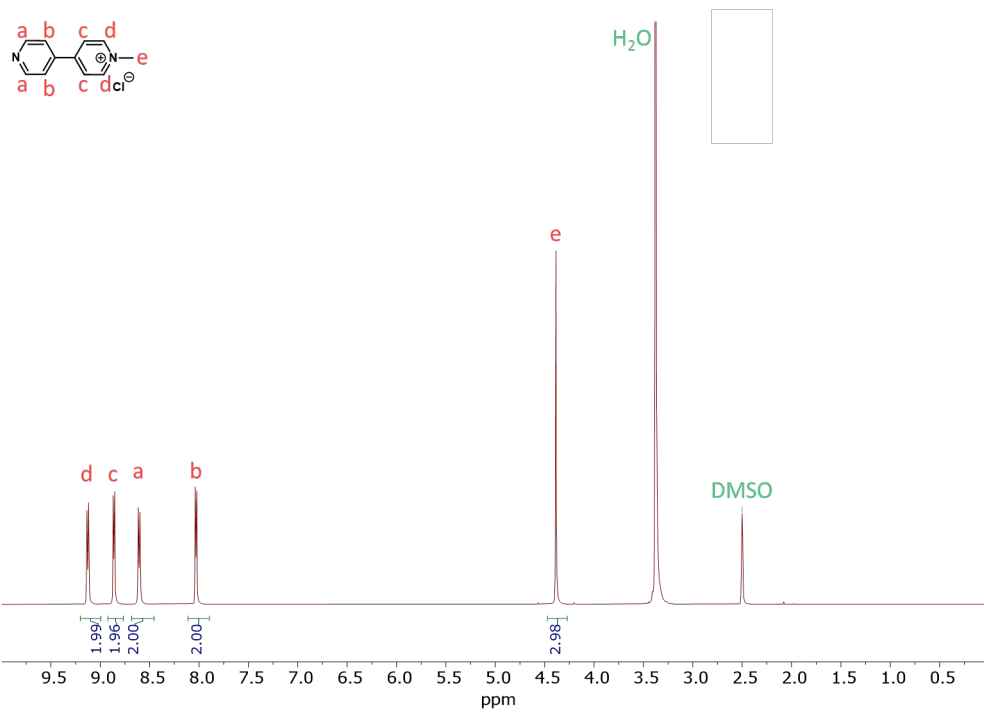
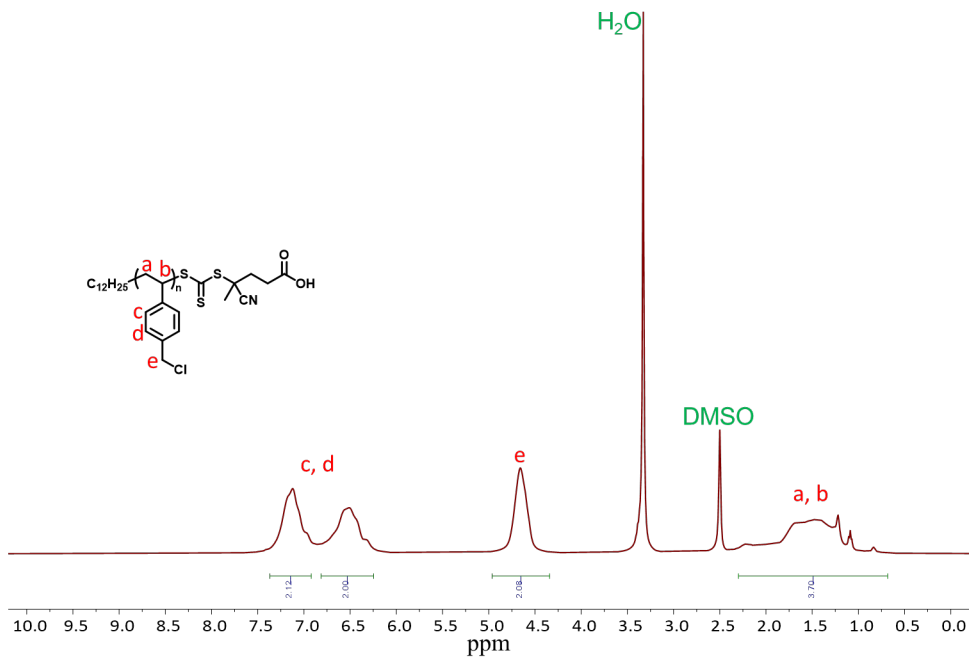


**Figure S12.**  $^1\text{H}$  NMR (400 MHz,  $\text{DMSO-}d_6$ ) of methyl viologen chloride (MV-Cl).

400 MHz - DMSO- $d_6$



101 MHz - DMSO- $d_6$

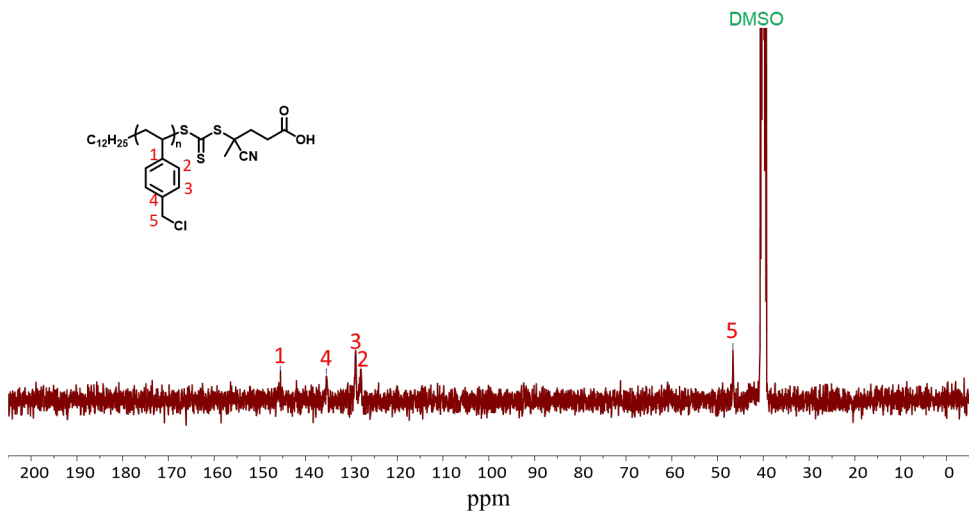


**Figure S13.**  $^1\text{H}$  NMR (400 MHz, DMSO- $d_6$ ) and  $^{13}\text{C}$  NMR (101 MHz, DMSO- $d_6$ ) spectra of poly(vinylbenzyl chloride) (PVBC).

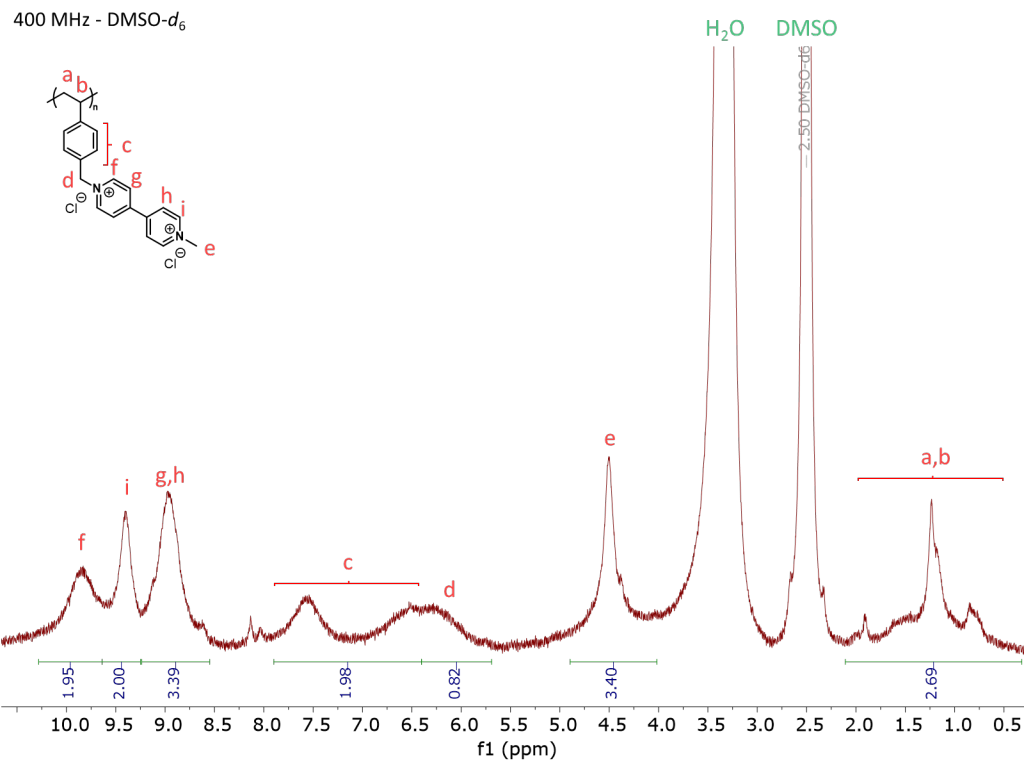


**Figure S14.**  $^1\text{H}$  NMR (400 MHz,  $\text{DMSO-}d_6$ ) of poly(vinylbenzyl methyl viologen) (PV).

**Table S1.** Elemental analysis of the synthesized polymers.

<b>Polymer</b>		<b>% C</b>	<b>% H</b>	<b>% N</b>	<b>% Cl</b>
PCPLG <sub>50</sub>	Calculated	47.01	5.97	6.85	N/A
	Found	47.29 (0.28)	5.97 (0.00)	6.68 (0.17)	N/A
PIPLG <sub>50</sub>	Calculated	32.67	4.15	4.76	N/A
	Found	32.44 (0.23)	4.02 (0.13)	4.51 (0.25)	N/A
Viol-C3-I	Calculated	38.48	3.93	7.07	N/A
	Found	38.33 (0.15)	4.36 (0.43)	6.47 (0.60)	N/A
Viol-C3-Cl	Calculated	55.43	5.67	10.19	17.08
	Calc'd (w/ 240 H <sub>2</sub> O)	45.87	6.62	8.43	14.13
	Found	45.85 (0.02)	5.98 (0.64)	7.72 (0.71)	10.52 (3.61)
PCNLG <sub>50</sub>	Calculated	58.11	8.38	4.88	N/A
	Found	60.16 (2.05)	8.33 (0.05)	4.92 (0.04)	N/A
PINLG <sub>50</sub>	Calculated	44.28	6.39	3.72	N/A
	Found	45.63 (1.35)	6.51 (0.12)	3.86 (0.14)	N/A
Viol-C9-I	Calculated	44.29	5.22	6.20	N/A
	Found	45.07 (0.78)	5.87 (0.65)	5.71 (0.49)	N/A
Viol-C9-Cl	Calculated	60.52	7.13	8.47	14.2
	Calc'd (w/ 220 H <sub>2</sub> O)	51.91	7.71	7.27	12.18
	Found	52.68 (0.77)	7.6 (0.11)	6.71 (0.56)	12.15 (0.03)
PVBC	Calculated	70.31	6.03	0.13	N/A
	Found	70.94 (0.63)	6.05 (0.02)	<0.1 %	N/A
PV	Calculated	66.7	5.65	7.73	19.42
	Calc'd (w/ 430 H <sub>2</sub> O)	50.1	7.03	5.80	14.57
	Found	50.94 (0.84)	4.54 (2.49)	5.31 (0.49)	10.62 (3.95)

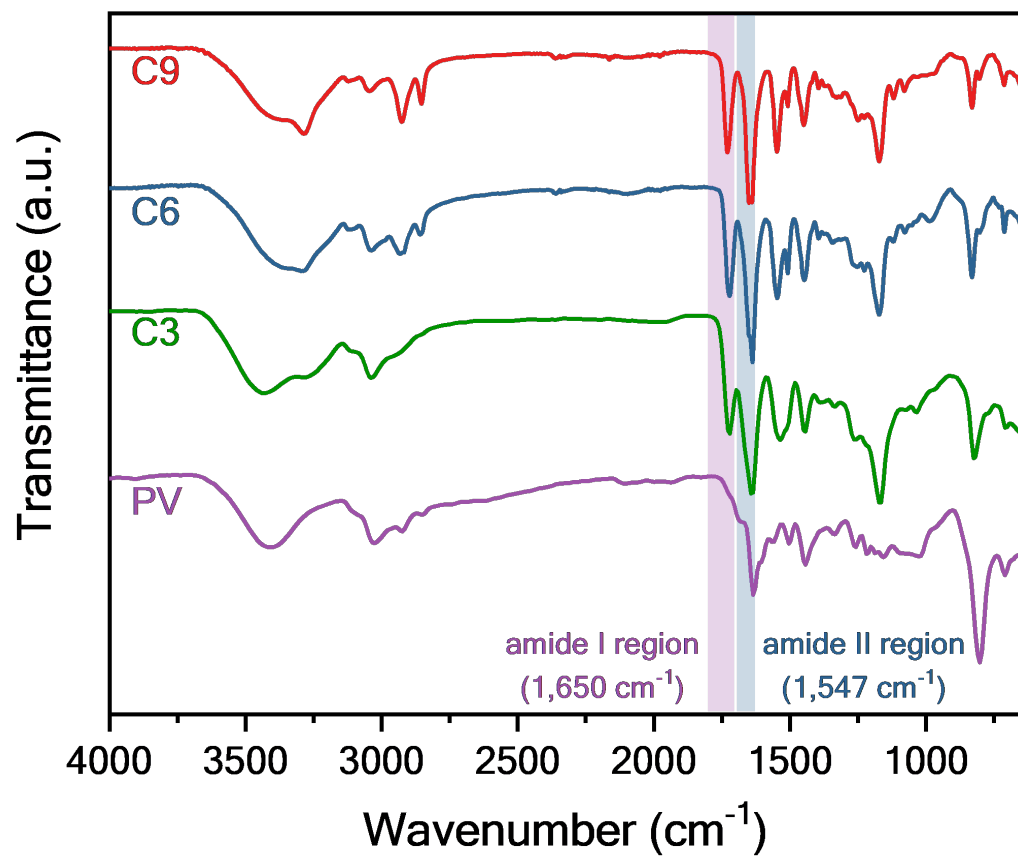


**Figure S15.** ATR-FTIR spectra for the C3, C6, and C9 viologen polypeptides and the control viologen polymer (PV).



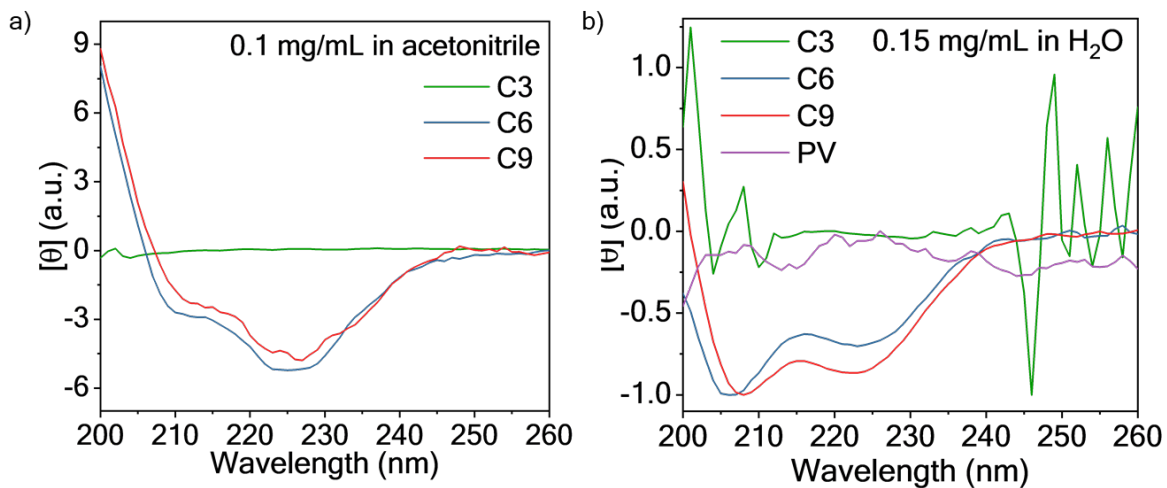
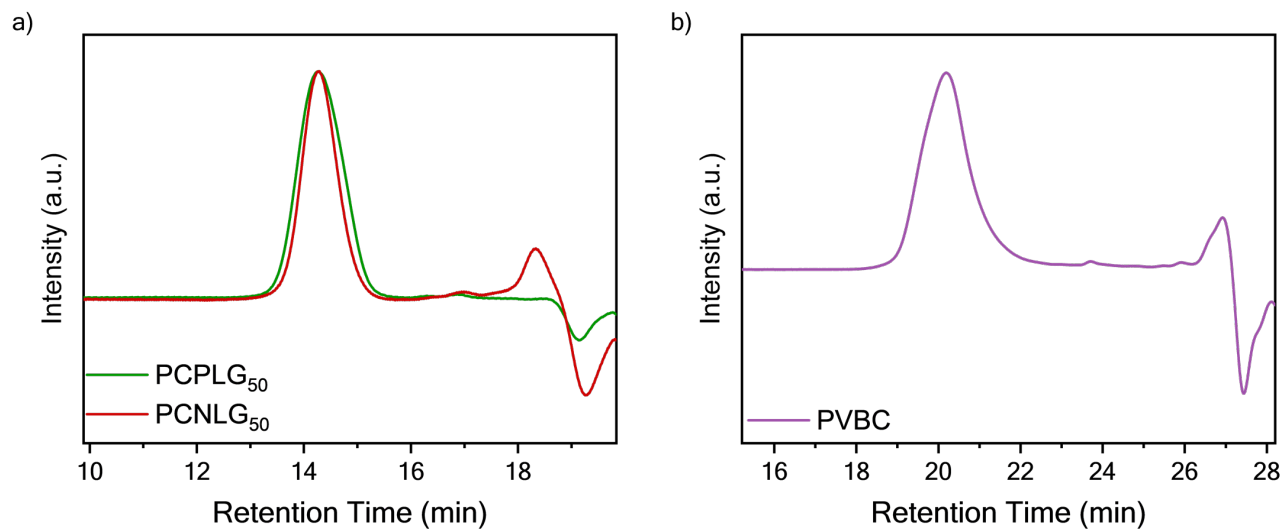


**Figure S16.** a) Normalized CD spectra for the **C3**, **C6**, and **C9** viologen polypeptides in acetonitrile and b) CD spectra for **C3**, **C6**, and **C9** and the control viologen polymer (**PV**) in H<sub>2</sub>O.



c)

Polymer	M/I	$M_n$ (kDa) <sup>a</sup>	$M_w$ (kDa) <sup>b</sup>	$M_n$ (kDa) <sup>b</sup>	$D^b$
PCPLG <sub>50</sub>	50:1	10.4	12.0	10.6	1.13
PCNLG <sub>50</sub>	50:1	14.6	13.6	12.4	1.10
PVBC	114:1	9.8	13.7	11.0	1.25

<sup>a</sup>Determined by <sup>1</sup>H NMR.

<sup>b</sup>Determined by DMF SEC unless otherwise noted.

<sup>c</sup>Determined by THF SEC.

**Figure S17.** a) DMF SEC traces for PCPLG<sub>50</sub> and PCNLG<sub>50</sub> or the precursors for **C3** and **C9** viologen polypeptides, respectively and b) THF SEC traces for PVBC or the precursor for **PV**. c) The corresponding tabulated dispersity and molar mass values for PCPLG<sub>50</sub>, PCNLG<sub>50</sub>, and PVBC.

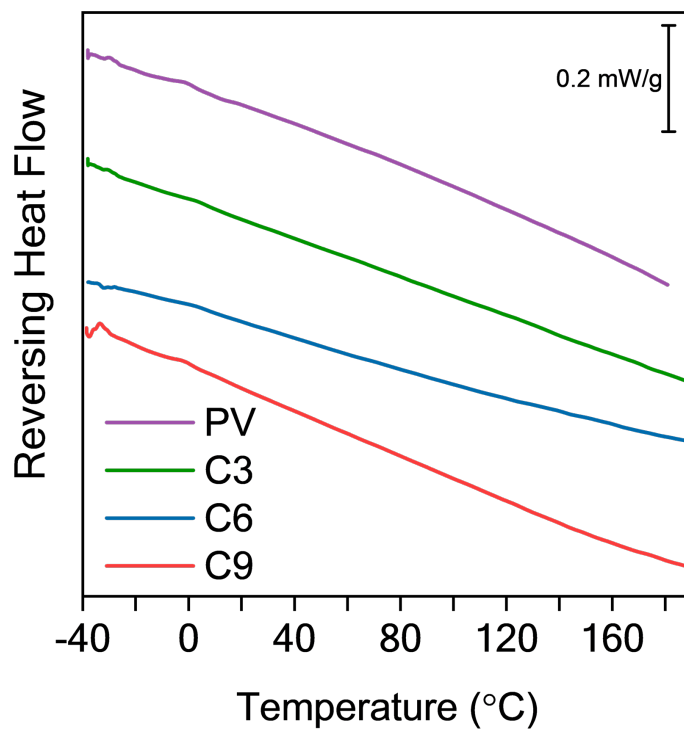


**Figure S18.** Modulated differential scanning calorimetry (MDSC) curves for the polymers studied. No thermal events were observed during the second MDSC heating cycles of the **C3**, **C6**, and **C9** viologen polypeptides and the control viologen polymer (**PV**). The samples were ramped from  $-40\text{ }^{\circ}\text{C}$  to  $200\text{ }^{\circ}\text{C}$  at a rate of  $5\text{ }^{\circ}\text{C}\cdot\text{min}^{-1}$  with amplitude of  $1.272\text{ }^{\circ}\text{C}$  for a period of 60 s with nitrogen purge at  $50\text{ mL}\cdot\text{min}^{-1}$ .

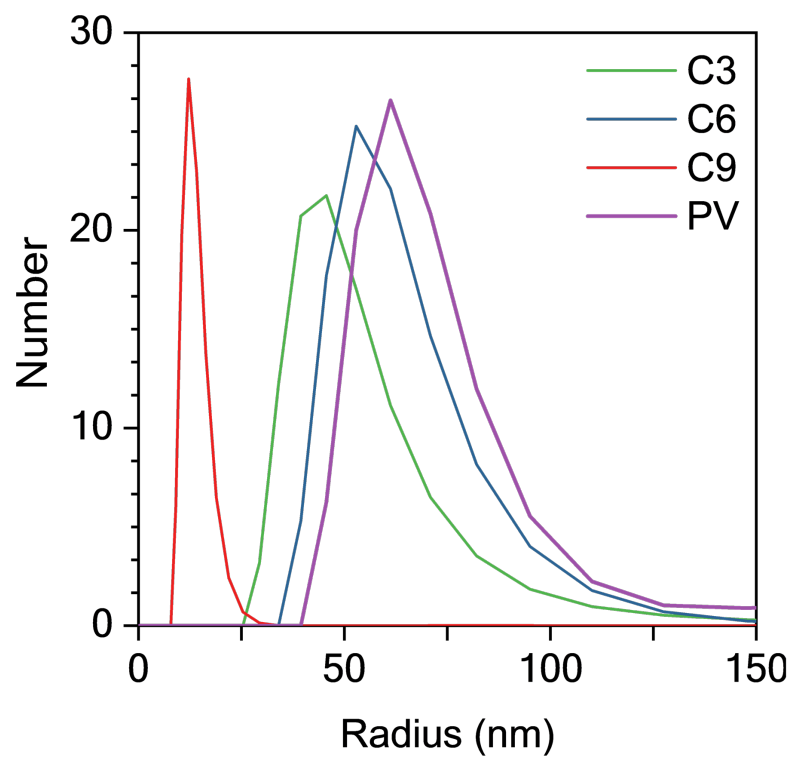


**Figure S19.** The number average hydrodynamic radius ( $r_h$ ) distribution of each polymer (0.3 mmol of repeating unit in water) obtained using DLS.

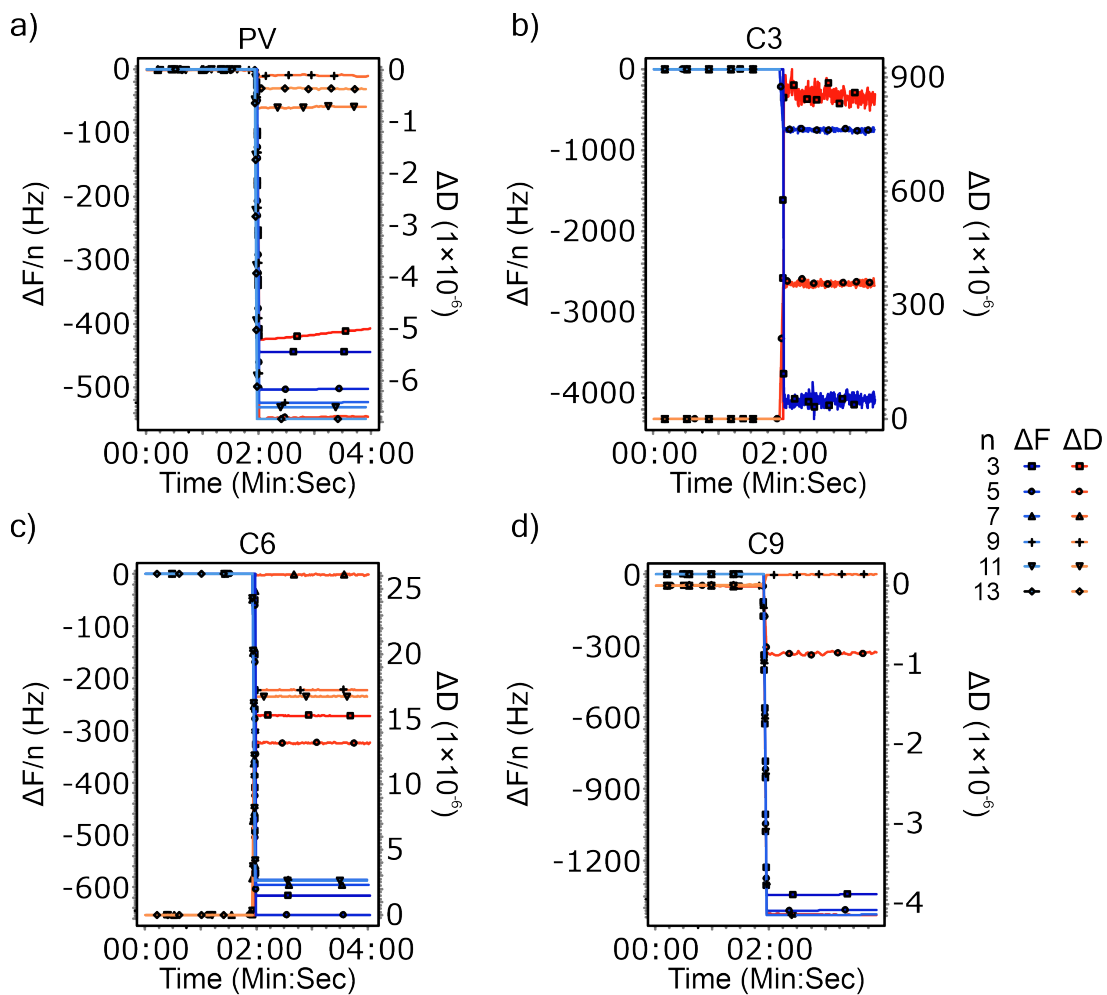


**Figure S20.** QCM-D overtone ( $n$ ) normalized frequency change ( $\Delta F/n$ ) and dissipation change ( $\Delta D$ ) for uncoated sensor (0 to 2 minutes) and polymer coated sensor (after 2 minutes) in air.  $\Delta F/n$  and  $\Delta D$  was collected for the 3, 5, 7, 9, 11, and 13<sup>th</sup> overtones of the fundamental frequency (1<sup>st</sup> overtone, 4.96 Hz). This data is fit using Sauerbrey equation to get the dry film thickness shown in **Figure S22**.

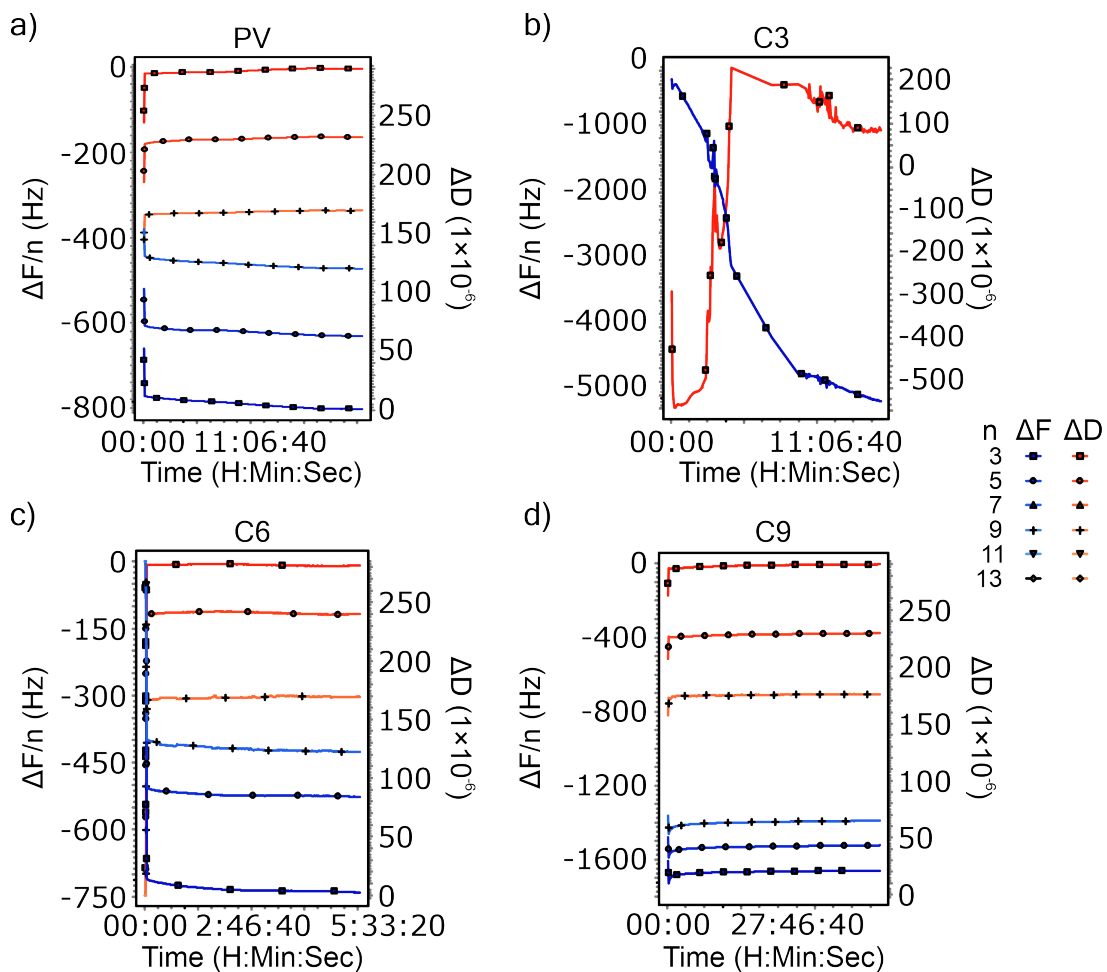


**Figure S21.** QCM-D raw overtone ( $n$ ) normalized frequency change ( $\Delta F/n$ ) and dissipation change ( $\Delta D$ ) for uncoated sensor (0 to 2 minutes) and polymer coated sensor (after 2 minutes) in 0.5 M LiCl in  $\gamma$ -butyrolactone.  $\Delta F/n$  and  $\Delta D$  was collected for the 3, 5, 7, 9, 11, and 13<sup>th</sup> overtones of the fundamental frequency (1<sup>st</sup> overtone, 4.96 Hz). This data is fit using Sauerbrey equation to get the swollen film thickness shown in Figure S22.

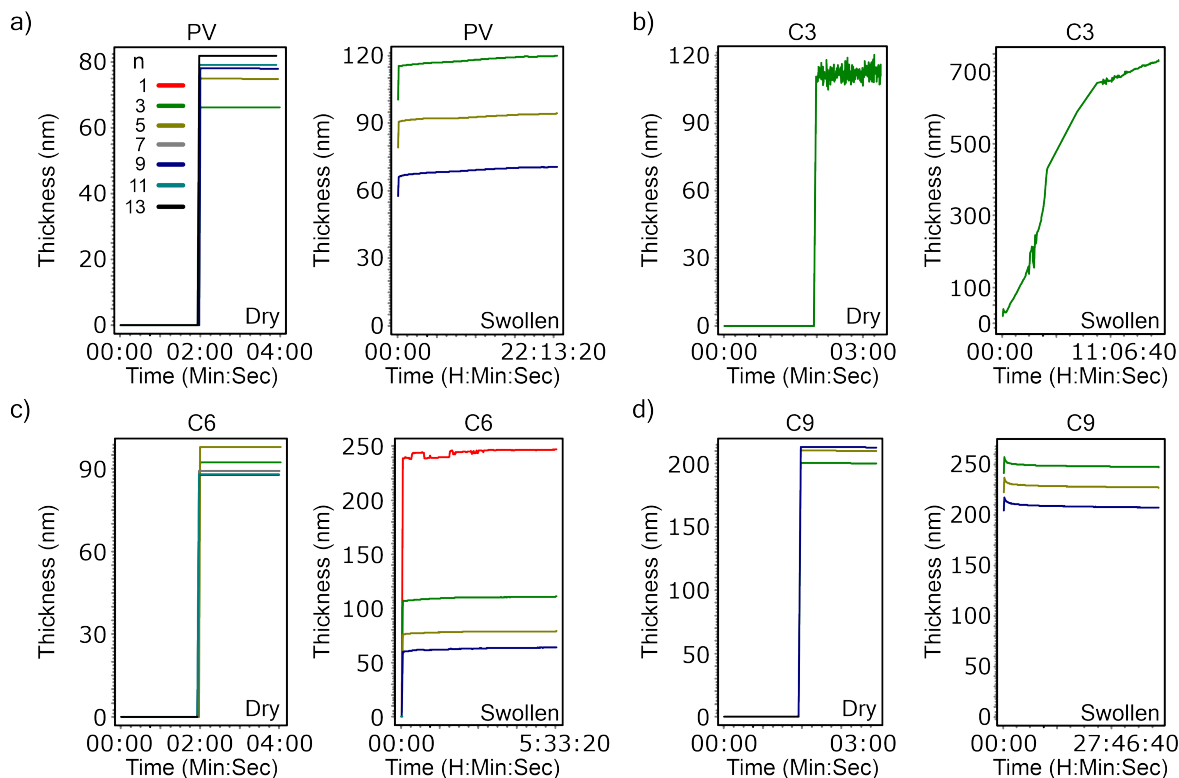


**Figure S22.** Dry and swollen thickness profiles from Sauerbrey fitting at each overtone ( $n$ ). The thickness swelling ratio is calculated using the dry thickness ( $h_{\text{dry}}$ ) and swollen thickness ( $h_{\text{swollen}}$ ) from the 3<sup>rd</sup> overtone.

**Table S2.** Summary of dry thickness ( $h_{\text{dry}}$ ), swollen thickness ( $h_{\text{swollen}}$ ), and thickness swelling ratio ( $Q_h$ ) determined using QCM-D. Sauerbrey fitting of the 3<sup>rd</sup> overtone results was used to determine  $h_{\text{dry}}$  and  $h_{\text{swollen}}$  are found in **Figures S22**. The raw QCM-D data is in **Figures S20** and **S21**.

Polymer	$h_{\text{dry}}$ (nm)	$h_{\text{swollen}}$ (nm)	$Q_h$
PV	66	119	1.80
C3	600	730	1.22
C6	92	111	1.21
C9	200	249	1.25

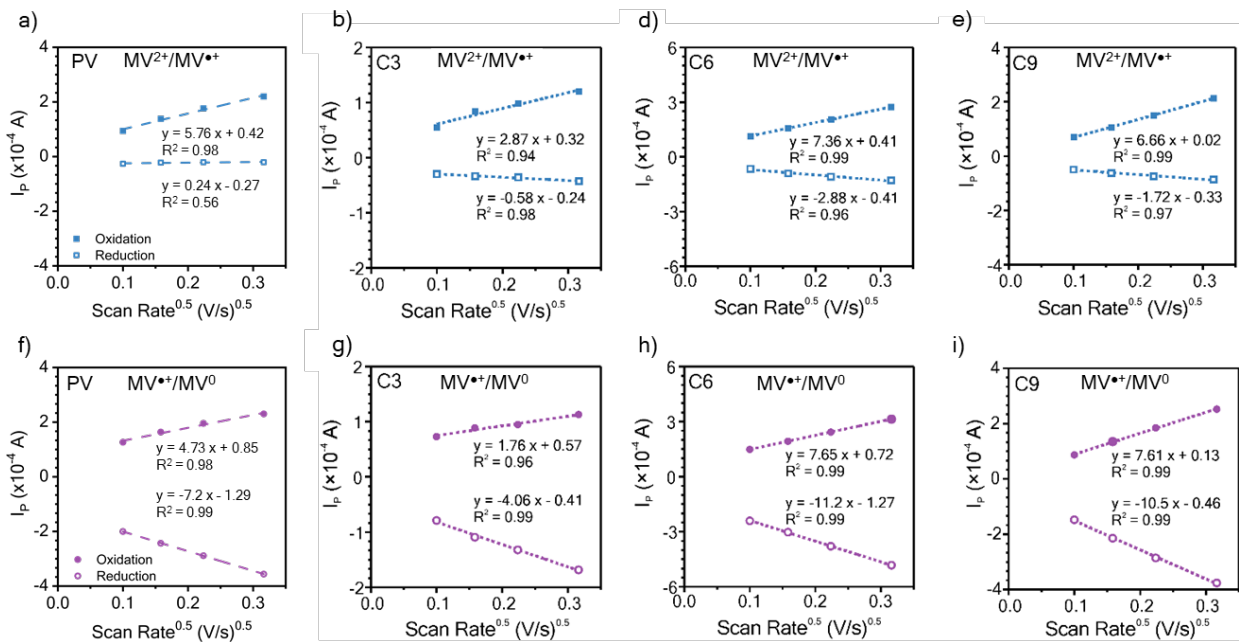


**Figure S23.** Peak current vs. square-root of scan rate from the cyclic voltammograms for **PV** (a,f), **C3** (b,g), **C6** (d,h), and **C9** (e,i).



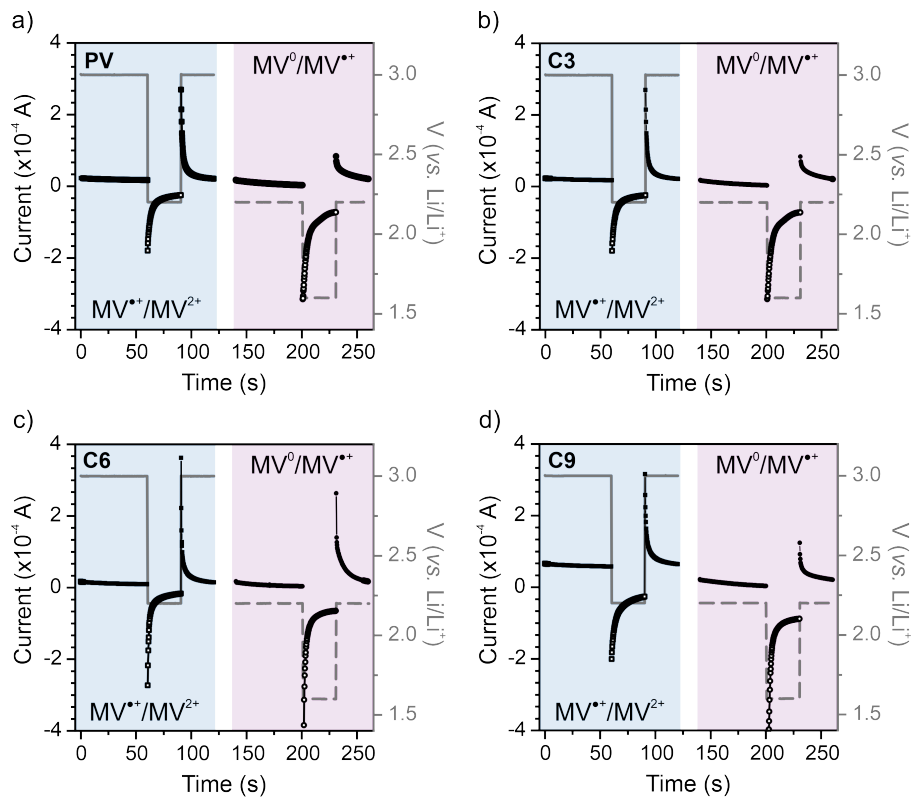


**Figure S24.** Chronoamperometry (CA) input and output data for a) PV, b) C3, c) C6, and d) C9.

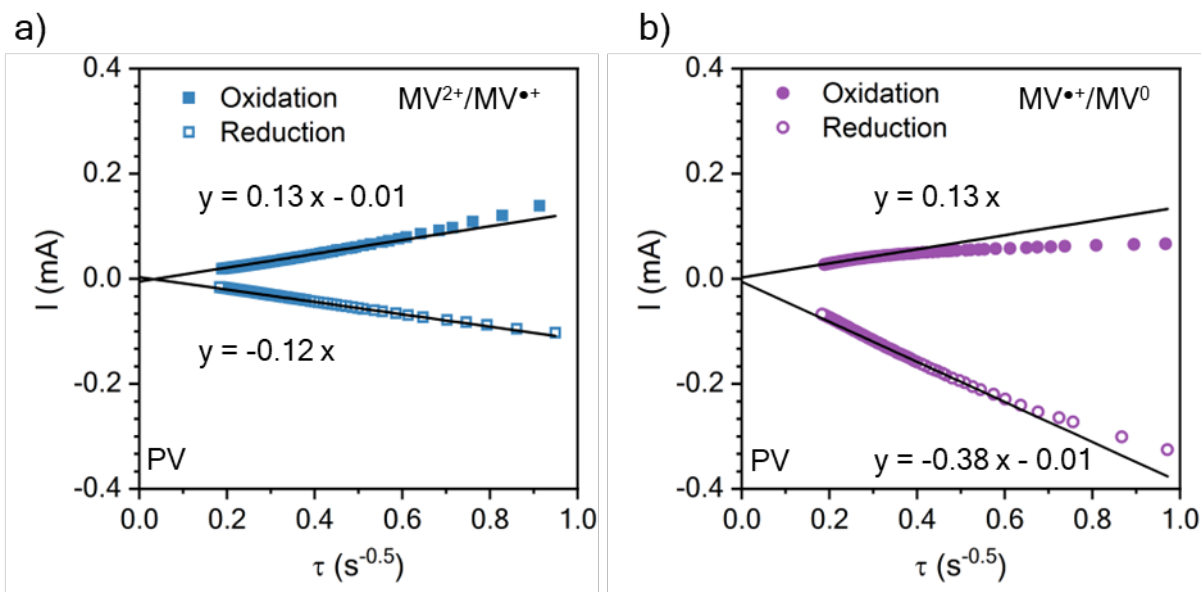


**Figure S25.** Chronoamperometry (CA) Cottrell plots for the two redox couples of the control viologen polymer (PV). a) shows the CA output data for the  $MV^{2+}/MV^{\bullet+}$  redox couple. b) shows the CA output data for the  $MV^{\bullet+}/MV^0$  redox couple. Polymer coated on ITO glass was used as the working electrodes in a three-electrode beaker cell configuration. The supporting electrolyte was 0.5 M LiCl in  $\gamma$ -butyrolactone. Lithium metal was used as counter and reference electrodes.

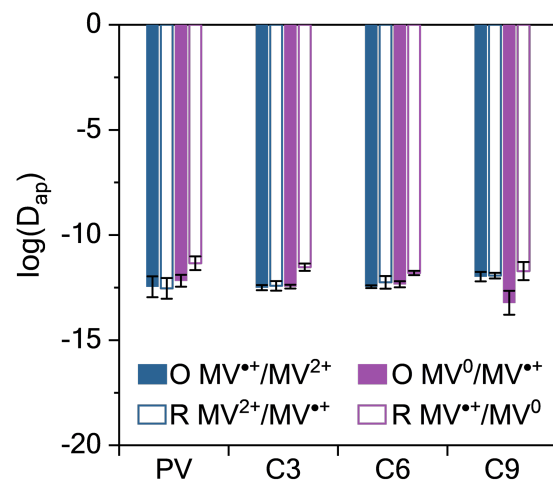


**Figure S26.**  $\log(D_{ap})$  values for the considered polymers. The values are separated for the oxidation and reduction of both redox couples.

## Discussion of trends for $k_{\text{ex}}$ and $k^0$ .

In the  $k_{\text{ex}}$  data, three main clusters appear (**Figure S27a-b**). The data in the red shaded area of **Figure S27a** was dominated by electrostatic repulsion of the  $\text{MV}^{2+}$  and/or the  $\text{MV}^{+}$  groups, which led to moderate  $k_{\text{ex}}$  values; the electrostatic repulsion between nearby groups may decrease  $k_{\text{ex}}$  by increasing the barrier to electron hopping. In the gray shaded region of **Figure S27b**, dimerization leads to ordering and close packing to facilitate rapid electron transfer, leading to the largest  $k_{\text{ex}}$  values. Finally, in the green shaded area in **Figure S27b**, C9 exhibited an entropy loss due to the dimerization which lead to slow electron transfer and the smallest  $k_{\text{ex}}$  value, likely from the longer linker improving the mobility of the viologen pendant and enabling more dimerization to occur. In contrast, C3, C6, and PV exhibited moderate  $k_{\text{ex}}$  values in the green shaded area, which were similar to the red shaded area  $k_{\text{ex}}$  values..

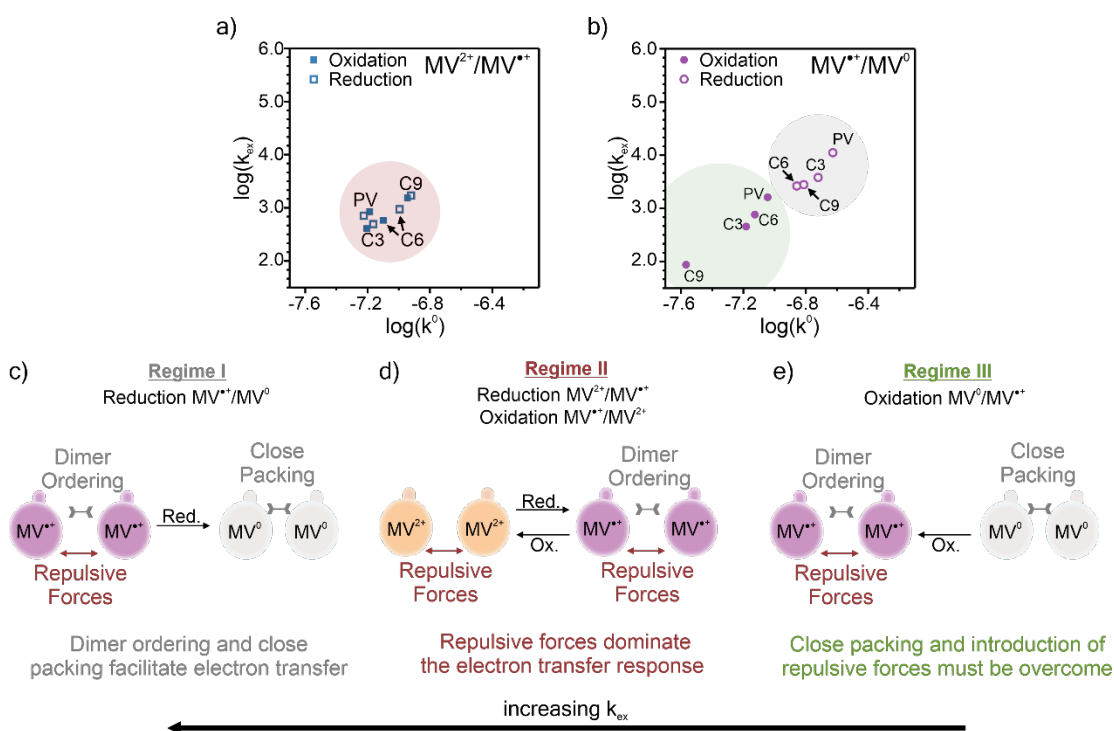


**Figure S27.** Summary of the  $\log(k_{\text{ex}})$  and  $\log(k^0)$  for PV, C3, C6, and C9. The results are presented as separate experimental values of oxidation and reduction for the a)  $\text{MV}^{2+}/\text{MV}^{+}$  and b)  $\text{MV}^{+}/\text{MV}^0$  redox couples. c - e) Schematic showing the relative  $k_{\text{ex}}$  values and the intermolecular forces between viologen groups in each regime.

### Determination of $k_{act}$ from Marcus-Hush Theory.

In addition to the dynamics of the polymer backbone and redox active groups in pendant RAPs, the electron hopping between redox centers needs to be considered to properly estimate  $k_{ex}$  and  $k^0$ . More explicitly, the electron transfer mechanism between methyl viologen groups is best represented by a consecutive reaction mechanism, such as between a donor (D) and an acceptor (A):



Equation S1

where  $k_{diff}$  is the diffusion-limited rate constant and  $k_{act}$  is the activation-limited rate constant.  $k_{act}$  can be determined from Marcus-Hush theory following:

$$k_{act} = K_a \left[ \left( -\frac{\pi}{\lambda k_b T} \right)^{1/2} \left( -\frac{H_{AB}^2}{\hbar} \right) \exp \left( -\frac{\Delta G^\ddagger}{k_b T} \right) \right]$$

Equation S2

where  $K_a$  is the association constant (*ca.* 0.38 M<sup>-1</sup> for viologen),<sup>3</sup>  $\lambda$  is the reorganization energy,  $k_b$  is the Boltzmann constant,  $T$  is temperature,  $H_{AB}$  is the electronic coupling,  $\hbar$  is the reduced Planck constant, and  $\Delta G^\ddagger$  is the activation energy for the transition state. For self-exchange electron transfer,  $\Delta G^\ddagger$  can be further approximated by  $(\lambda - 2H_{AB})^2 / 4\lambda$ .<sup>4</sup> To calculate  $k_{act}$ ,  $H_{AB}$  and  $\lambda$  were first determined by DFT methods.

For determining  $H_{AB}$ , it is important to consider the adjacent pendant viologen position. Two axes were adopted to represent the position of adjacent viologens: 1) the height axis and 2) the displacement axis, where the height axis was plane-to-plane distance and the displacement axis was plane offset (**Figure S28a**). From the simulations, it was observed that electronic coupling between MV<sup>2+</sup>/MV<sup>•+</sup> and MV<sup>•+</sup>/MV<sup>0</sup> (with a fixed height of 3.5 Å) behaved differently along the displacement, due to different molecular orbital interactions (**Figure S28b**). However, at ideal positions between adjacent methyl viologens, electronic coupling between MV<sup>2+</sup>/MV<sup>•+</sup> and MV<sup>•+</sup>/MV<sup>0</sup> are nearly identical (**Figure S28c**). The data from **Figure S28c** can be further fitted by exponential curves, which is consistent with the quantum mechanical interpretation of decreasing orbital overlap. Electronic coupling for the dimers obtained from snapshots at different oxidation states (**Figure S28d-e**) followed similar trends to the values for dimers with no displacement (**Figure S28c**). An example snapshot is shown in **Figure S29**.

The calculation of  $\lambda$  is error prone and high precision is required due to the exponential relationship to  $k_{ex}$  (i.e. a small change in the reorganization energy will result in large difference  $k_{ex}$ ). To correctly capture the subtlety of calculating  $\lambda$ , we utilized LC- $\omega$ HPBE which includes a range-separated and dispersion-corrected method. The calculations resulted in estimates of the total reorganization energy between MV<sup>2+</sup>/MV<sup>•+</sup> and MV<sup>•+</sup>/MV<sup>0</sup> of 1.65 and 1.31 eV, respectively.

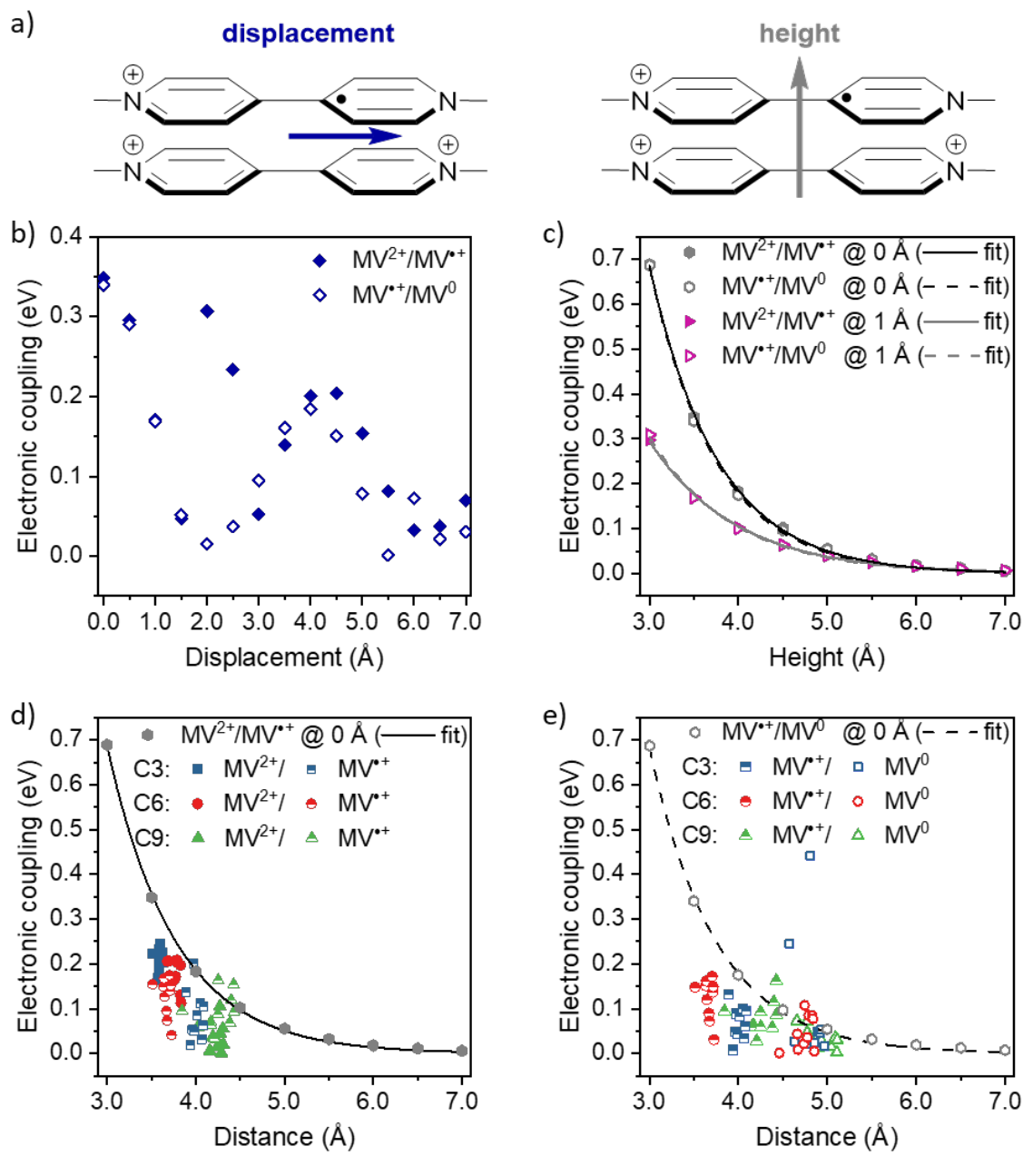


**Figure S28.** a) Diagram of the displacement and height axis for the viologen groups. b) Electronic coupling ( $H_{AB}$ ) values between  $MV^{2+}/MV^{\bullet+}$  and  $MV^{\bullet+}/MV^0$  along the displacement axis at 3.5 Å height. Electronic coupling values between c)  $MV^{2+}/MV^{\bullet+}$  and  $MV^{\bullet+}/MV^0$  at ideal positions along the height axis at 0 Å displacement and 1 Å displacement. Electronic coupling values between d)  $MV^{2+}/MV^{\bullet+}$  and e)  $MV^{\bullet+}/MV^0$  dimers from different simulation snapshots along the height axis with 0 Å displacement.

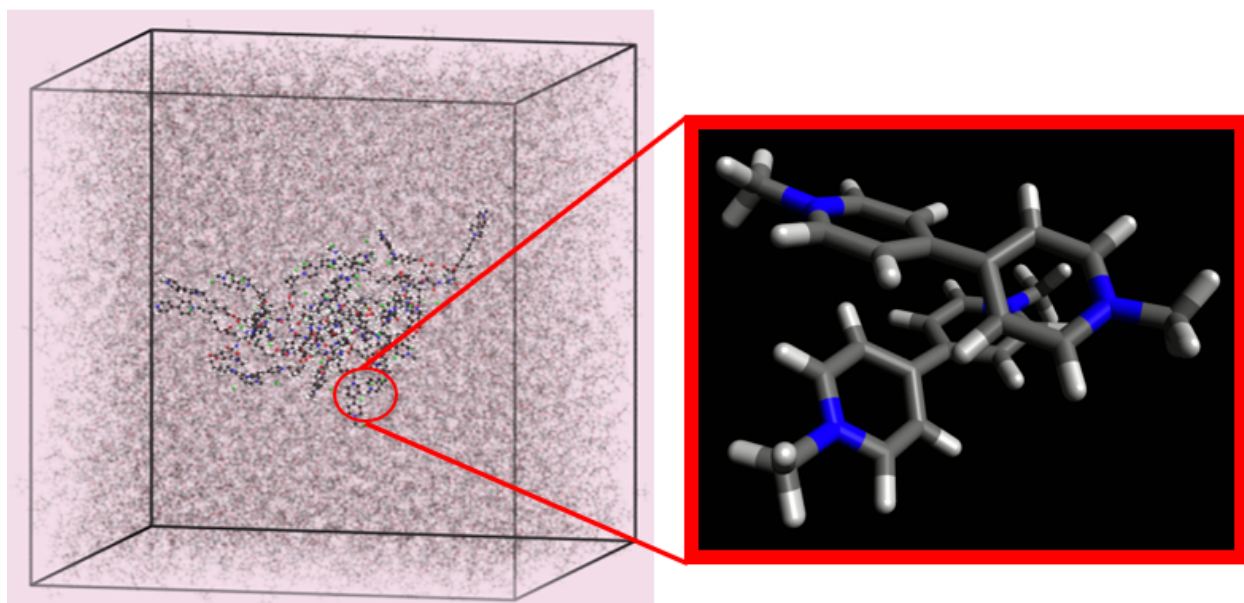
**Table S3.** Experimentally determined  $\log(k_{\text{ex}})$  (L/ mol s) values from chronoamperometry (CA), using **Equation 2**, for reduction and oxidation of both redox couples.

	$\log(k_{\text{ex}})$			
	$\text{MV}^{2+}/\text{MV}^{•+}$		$\text{MV}^{•+}/\text{MV}^0$	
	<b>Oxidation</b>	<b>Reduction</b>	<b>Oxidation</b>	<b>Reduction</b>
<b>PV</b>	$2.9 \pm 0.49$	$3.2 \pm 0.28$	$2.9 \pm 0.49$	$4.1 \pm 0.33$
<b>C3</b>	$2.6 \pm 0.12$	$2.7 \pm 0.23$	$2.7 \pm 0.09$	$3.6 \pm 0.17$
<b>C6</b>	$2.8 \pm 0.06$	$3.0 \pm 0.30$	$2.9 \pm 0.14$	$3.4 \pm 0.10$
<b>C9</b>	$3.2 \pm 0.22$	$3.2 \pm 0.14$	$1.9 \pm 0.57$	$3.5 \pm 0.43$

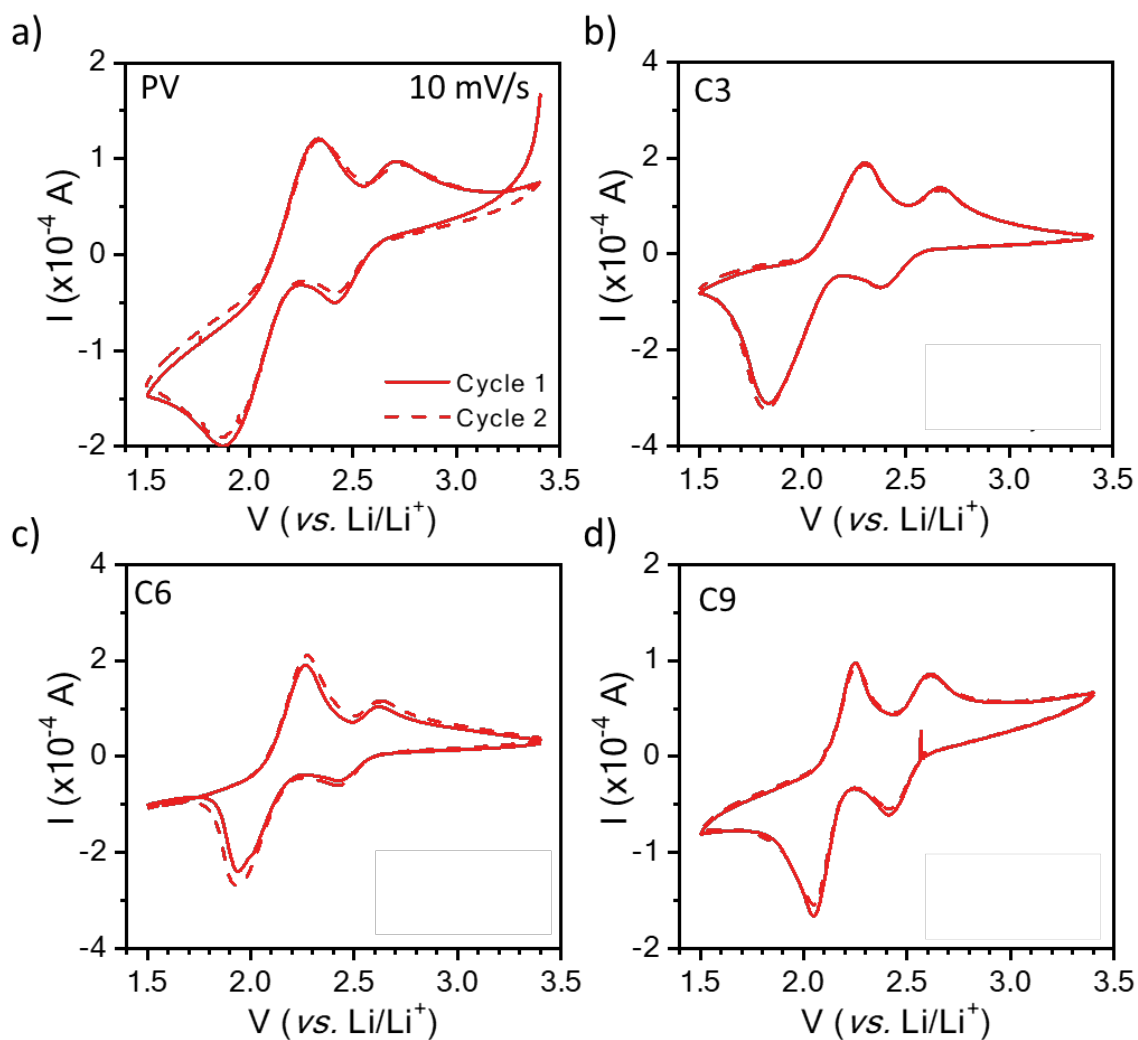
**Table S4.** Experimentally determined  $\log(k^0)$  (cm/s) values from cyclic voltammetry peak separation ( $\Delta E_p$ ), using **Equation 4**, for reduction and oxidation of both redox couples.

	$\log(k^0)$			
	$MV^{2+}/MV^{•+}$		$MV^{•+}/MV^0$	
	<b>Oxidation</b>	<b>Reduction</b>	<b>Oxidation</b>	<b>Reduction</b>
<b>PV</b>	$-7.2 \pm 0.25$	$-7.2 \pm 0.25$	$-7.0 \pm 0.14$	$-6.6 \pm 0.16$
<b>C3</b>	$-7.2 \pm 0.06$	$-7.2 \pm 0.11$	$-7.2 \pm 0.05$	$-6.7 \pm 0.09$
<b>C6</b>	$-7.1 \pm 0.12$	$-7.0 \pm 0.14$	$-7.1 \pm 0.07$	$-6.9 \pm 0.05$
<b>C9</b>	$-6.9 \pm 0.11$	$-6.9 \pm 0.07$	$-7.6 \pm 0.28$	$-6.8 \pm 0.22$

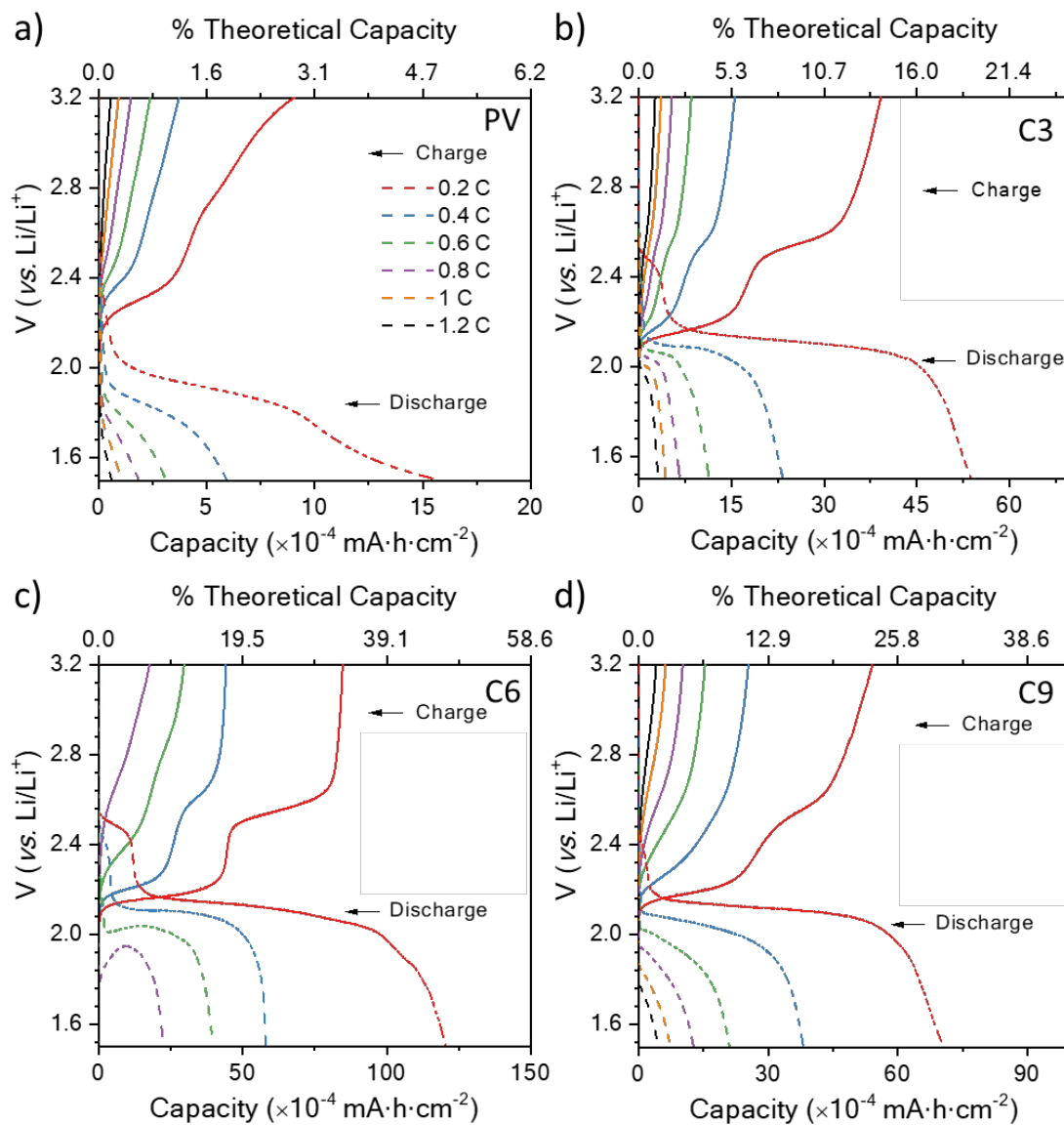




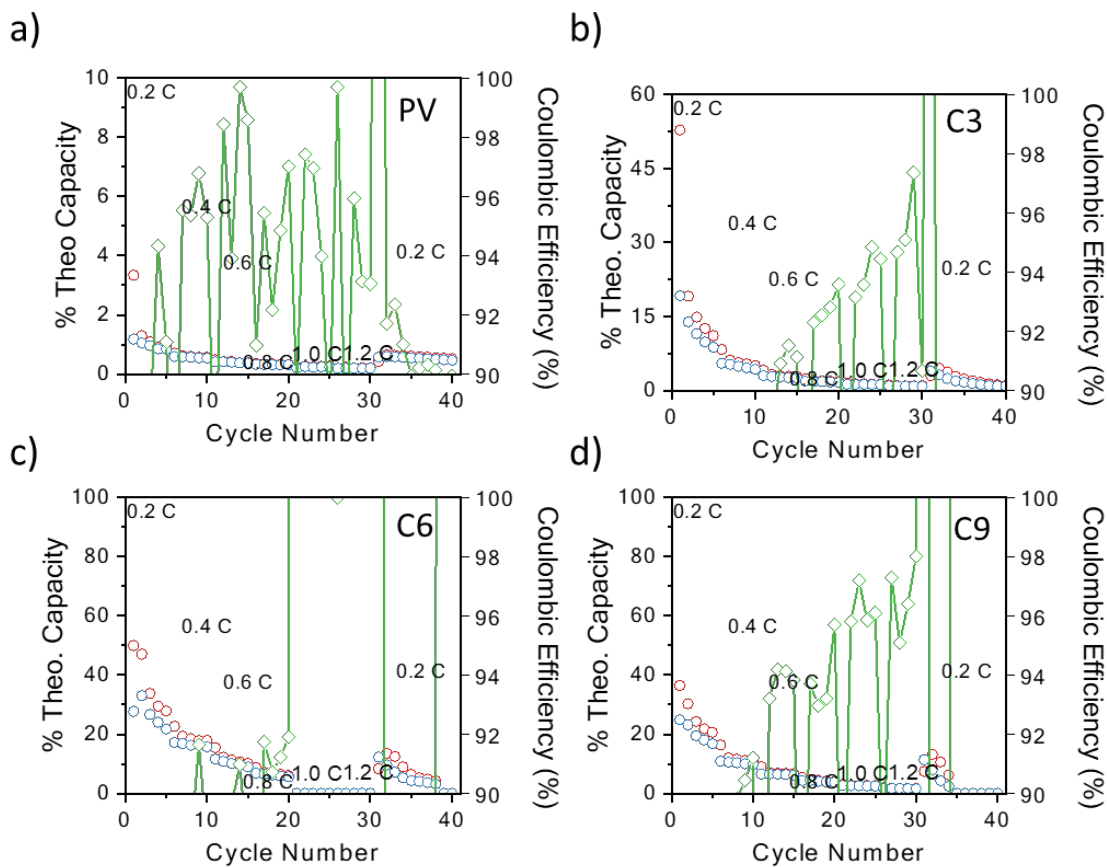
**Figure S29.** Snapshot of a pair of methyl viologen from an oligomer simulation.



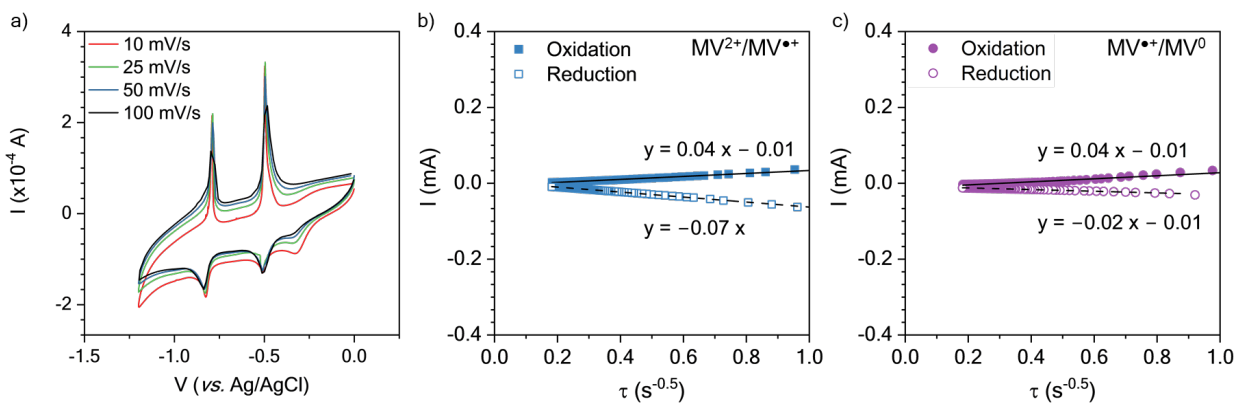
**Figure S30.** Cyclic voltammograms of a half-sandwich cell a) **PV**, b) **C3**, c) **C6**, and d) **C9**. The working electrode was a thin film on ITO glass in a half cell with lithium metal. The separator was filter paper soaked in 0.5 M LiCl in GBL electrolyte.



**Figure S31.** Galvanostatic charge-discharge curves for the a) PV, b) C3, c) C6, and d) C9 half cells against lithium metal. The working electrode was a polymer thin film on ITO-coated glass and 0.5 M LiCl in GBL on filter paper as the supporting electrolyte and separator, respectively.

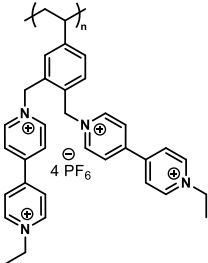
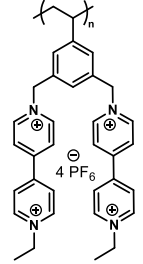
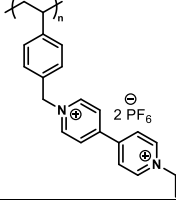
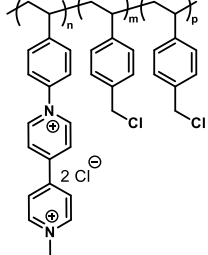
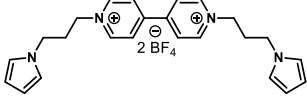
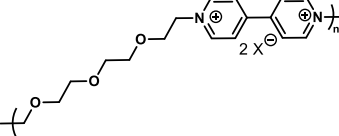
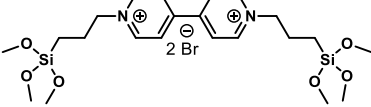


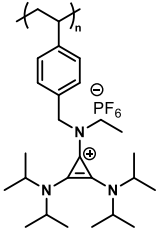
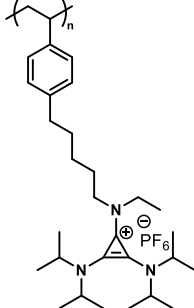
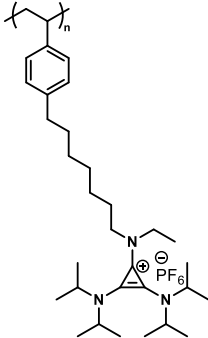
**Figure S32.** GCD Summary plots of a half-sandwich cell for a) **PV**, b) **C3**, c) **C6** and d) **C9**. The working electrode was a thin film on ITO glass in a half cell with lithium metal. The separator was filter paper soaked in 0.5 M LiCl in GBL electrolyte.



**Figure S33.** a) Cyclic voltammograms at 10, 25, 50, and 100  $mV \cdot s^{-1}$  for a 0.2 mM solution of C6 dissolved in 0.5 M NaCl in  $H_2O$  supporting electrolyte. Chronoamperometry (CA) Cottrell plots for b) for the  $MV^{2+}/MV^{•+}$  redox couple and c) the  $MV^{•+}/MV^0$  redox couple. The CV and CA experiments were conducted in a three-electrode beaker cell configuration with a glassy carbon working electrodes, a platinum wire counter electrode, and a Ag/AgCl (sat.) reference electrode.

**Table S4.** Summary of kinetic parameters for previous viologen polymers studied in literatures.  $C_0^*$  is the total concentration of redox sites (or repeat units in mol/cm<sup>3</sup>).

Polymer Structure	$C_0^*$	Log( $k_{ex}$ )	Log( $k^0$ )	Log( $D_{et}$ )	Ref.
	NA	5.23 <sup>a</sup>	-6.96	-10.39	5c
	NA	4.95 <sup>a</sup>	-6.78	-10.60	5c
	NA	4.12 <sup>a</sup>	-6.00	-10.10	5c
	NA	5.2 <sup>a</sup>	-5	NA	6c
	4.5 M	3.9	NA	-10.72 (MV <sup>2+</sup> /MV <sup>•+</sup> )	7b
		5.2	NA	-8.82 (MV <sup>•+</sup> /MV <sup>0</sup> )	
	NA	7.04	NA	-7.52	8c
	NA	7.95	NA	-6.52	
	0.74 M	5.90	NA	-9.52	9

	10 mM	NA	-3.12	-5.65	10
	10 mM	NA	-3.11	-5.84	
	10 mM	NA	-3.09	-5.96	

<sup>a</sup>Only the MV<sup>+</sup>/MV<sup>0</sup> redox couple is studied for thin films

<sup>b</sup>Value determined from reduction only

<sup>c</sup>Not stated if value is determined from oxidation or reduction

## REFERENCES

- (1) Nguyen, T. P.; Easley, A. D.; Kang, N.; Khan, S.; Lim, S.-M.; Rezenom, Y. H.; Wang, S.; Tran, D. K.; Fan, J.; Letteri, R. A.; He, X.; Su, L.; Yu, C.-H.; Lutkenhaus, J. L.; Wooley, K. L. Polypeptide Organic Radical Batteries. *Nature* **2021**, *593* (7857), 61–66. <https://doi.org/10.1038/s41586-021-03399-1>.
- (2) Nagarjuna, G.; Hui, J.; Cheng, K. J.; Lichtenstein, T.; Shen, M.; Moore, J. S.; Rodríguez-López, J. Impact of Redox-Active Polymer Molecular Weight on the Electrochemical Properties and Transport Across Porous Separators in Nonaqueous Solvents. *J. Am. Chem. Soc.* **2014**, *136* (46), 16309–16316. <https://doi.org/10.1021/ja508482e>.
- (3) Neta, P.; Richoux, M.-C.; Harriman, A. Intramolecular Association of Covalently Linked Viologen Radicals. *J. Chem. Soc., Faraday Trans. 2* **1985**, *81* (9), 1427–1443. <https://doi.org/10.1039/F29858101427>.
- (4) Ohsaka, T.; Yamamoto, H.; Oyama, N. Thermodynamic Parameters for Charge-Transfer Reactions in Pendant Viologen Polymers Coated on Graphite Electrodes and at Electrode/Pendant Viologen Polymer Film Interfaces. *The Journal of Physical Chemistry* **1987**, *91* (14), 3775–3779. <https://doi.org/10.1021/j100298a012>.
- (5) Burgess, M.; Chénard, E.; Hernández-Burgos, K.; Nagarjuna, G.; Assary, R. S.; Hui, J.; Moore, J. S.; Rodríguez-López, J. Impact of Backbone Tether Length and Structure on the Electrochemical Performance of Viologen Redox Active Polymers. *Chemistry of Materials* **2016**, *28* (20), 7362–7374. <https://doi.org/10.1021/acs.chemmater.6b02825>.
- (6) Sato, K.; Ichinoi, R.; Mizukami, R.; Serikawa, T.; Sasaki, Y.; Lutkenhaus, J.; Nishide, H.; Oyaizu, K. Diffusion-Cooperative Model for Charge Transport by Redox-Active Nonconjugated Polymers. *Journal of the American Chemical Society* **2018**, *140* (3), 1049–1056. <https://doi.org/10.1021/jacs.7b11272>.
- (7) Dalton, E. F.; Murray, R. W. Viologen(2+/1+) and Viologen(1+/0) Electron-Self-Exchange Reactions in a Redox Polymer. *The Journal of Physical Chemistry* **1991**, *95* (16), 6383–6389. <https://doi.org/10.1021/j100169a056>.
- (8) Terrill, R. H.; Hutchison, J. E.; Murray, R. W. Solid State Electron-Hopping Transport and Frozen Concentration Gradients in a Mixed Valent Viologen–Tetraethylene Oxide Copolymer. *J. Phys. Chem. B* **1997**, *101* (9), 1535–1542. <https://doi.org/10.1021/jp962614p>.
- (9) Gaudiello, J. G.; Ghosh, P. K.; Bard, A. J. Polymer Films on Electrodes. 17. The Application of Simultaneous Electrochemical and Electron Spin Resonance Techniques for the Study of Two Viologen-Based Chemically Modified Electrodes. *J. Am. Chem. Soc.* **1985**, *107* (11), 3027–3032. <https://doi.org/10.1021/ja00297a006>.
- (10) Montoto, E. C.; Cao, Y.; Hernández-Burgos, K.; Sevov, C. S.; Braten, M. N.; Helms, B. A.; Moore, J. S.; Rodríguez-López, J. Effect of the Backbone Tether on the Electrochemical Properties of Soluble Cyclopropenium Redox-Active Polymers. *Macromolecules* **2018**, *51* (10), 3539–3546. <https://doi.org/10.1021/acs.macromol.8b00574>.



